# Communications of the
# LUNAR AND PLANETARY
# LABORATORY

Communications Nos. 166–171
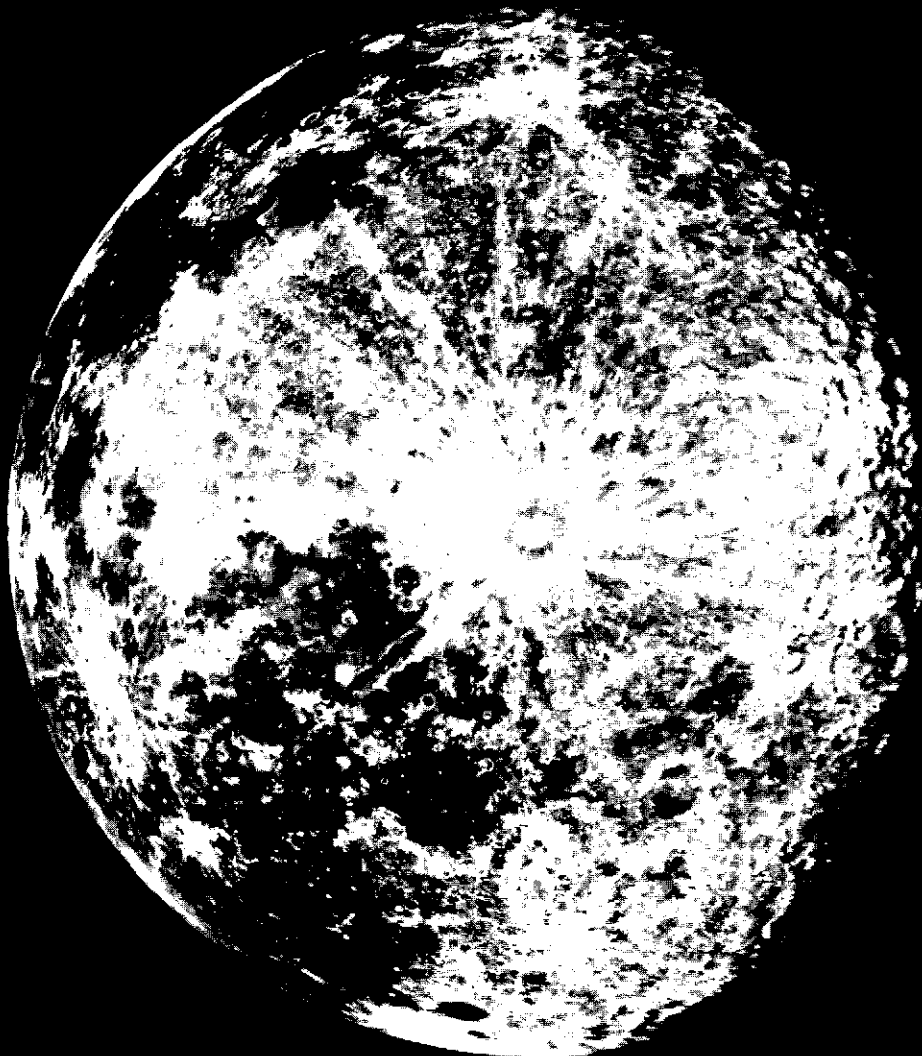
Volume 9    Part 3

# THE UNIVERSITY OF ARIZONA

# Communications of the
# LUNAR AND PLANETARY
# LABORATORY

## Communications of the Lunar and Planetary Laboratory

These *Communications* contain the shorter publications and reports by the staff of the Lunar and Planetary Laboratory. They may be either original contributions, reprints of articles published in professional journals, preliminary reports, or announcements. Tabular material too bulky or specialized for regular journals is included if future use of such material appears to warrant it. The *Communications* are issued as separate numbers, but they are paged and indexed by volumes.

The *Communications* are mailed to observatories and to laboratories known to be engaged in planetary, interplanetary or geophysical research in exchange for their reports and publications. The University of Arizona Press can supply at cost copies to other libraries and interested persons.

## TABLE OF CONTENTS

# No. 166 ARIZONA-NASA ATLAS OF THE INFRARED SOLAR SPECTRUM, REPORT X

*by* D. C. BENNER, G. P. KUIPER, L. RANDIĆ, AND A. B. THOMSON

May 1, 1970

## ABSTRACT

This report concludes the series of the Arizona-NASA Infrared Solar Spectrum Atlas; it follows *LPL Comm.* No. 162 (which contains Charts B1-B9) and thereby completes the B series. The wavelength interval covered is 13350-34100 Å.

The present paper contains the second and last set of B-spectrometer records, obtained on the NASA CV-990, July 1968, with a 600-line per mm grating. There is a small overlap with the 1200 line/mm records; B9 terminates at 14098 Å, whereas the present series begins at 13350 Å. The value of the present series lies primarily in serving as reference to high-altitude planetary spectra taken with similar resolutions, 6-10,000. The 4-meter records, with their 4X higher resolution, give a more detailed and valuable description of the solar spectrum as such and, incidentally, assist in the interpretation of the intensity tracings here reproduced. Because of inherent uncertainties in spectrometer traces recorded in flight, the present records contain valuable checks on the solar and telluric spectra published before.

The wavelength scale and the classification of absorption lines are taken from the 4-meter spectra. For the interval 13350-28500 Å, two good independent B records were available and are here reproduced. For the 28500-34000 Å, mostly only one good record was available, with the second set used only to verify the set here published. For the 3.3 $\mu$ region ($\nu_3$ of $CH_4$) a B-spectrometer trace had already been reproduced in *LPL Comm.* No. 125, page 223 (having slightly better resolution).

Table I contains the relevant data on each of the charts. In some spectra the continuum has a somewhat wavy appearance (e.g. on B15), due either to minor interference effects in the optical train (possibly a thin filter so oriented as to cause the double reflection to strike the detector); or else,

to minor guiding errors (guiding was on the center of the solar disk but occasional uncompensated motions of the aircraft caused the solar image on the slit to shift. An extreme case on B13 at 17500 Å has been marked "g"). On B13-16 and B19 some cases occur of lines slightly displaced and distorted (apparently due to a sharply localized defect in the grating drive that may show its appearance after one or more revolutions, some 480 Å apart); they are marked "b" and are not marked "real" (dot below) if displaced (in such a case a real solar line will be missing among the numbered lines). On B12 and B13, $a$ and $b$, the 1 $\mu$ filter (Corning 2540) was used, causing a minor second-order leak near 1.8 $\mu$, similar to that discussed for the 4-meter records, *LPL Comm.* No. 163, p. 66. Attention is drawn to P $\alpha$ on B13, still cut by telluric $H_2O$. Good records were obtained of the three telluric $CO_2$ bands at 2 $\mu$ and the two stronger bands at 2.69 and 2.77 $\mu$ (including isotopic components).

Identifications have been added where deemed useful. As in the other Reports, all absorptions regarded real, either solar or telluric, are indicated by dots *below* the traces, numbered consecutively for future reference. Dots *above* the traces designate telluric $H_2O$ absorptions; open triangles, $CH_4$; short vertical lines, $CO_2$; crossed open circles, $N_2O$; and asterisks, CO. Solar identifications are added where known and considered appropriate. Partial contributions, in excess of ¼ of the total intensity, are placed in parentheses.

### ERRATA IN REPORTS I - IX

In the preparation of Report X ($\lambda > 13400$A), a few rather minor errata were detected in the earlier reports, which are listed below. The verification was not exhaustive but indicates very few errors among the thousands of identifications.

| CHART | LINE | CORRECTION |
|---|---|---|
| 25a | 30 | not $H_2O$ |
| 25d | 30 | partly $H_2O$ |
| 26a | 5 | $H_2O$ |
| 26a | 20 | $H_2O$ |
| 26a | 77 | $H_2O$ |
| 26a | 84 | $H_2O$ |
| 26a | 97 | not $H_2O$ |
| 27b | 29 | partly $H_2O$ |
| 27b | 35 | $H_2O$ |
| 34d | 19, 21 | not $H_2O$ |
| 34d | 54 | omit (:) |
| 38a | 75 | add · below |
| 39a | 28 | omit (|) |
| 47c | 10 | add ($\nabla$) |
| B8c | 5 | add ⊙ |
| B9c, d | 2 | partly $H_2O$ |
| B9c, d | 22 | omit () |
| B9c | 39 | $H_2O$ |
| B9c | 48 | omit () |

## TABLE I

SOLAR SPECTRUM RECORDS, B-SPECTROMETER, NASA CV-990 JET

2.5 μ GRATING (600 LINES/MM), SLIT AND CELL 0.10 MM, $\tau = 0.12$, 2 μ FILTERS

| FIG. | CHART | λ(Å) | 1968 DATE | UT | ALT. (FT.) | OUTSIDE TEMP. (°C) | CABIN ALT. (FT.) | GAIN |
|---|---|---|---|---|---|---|---|---|
| 1 | B10 a* | 13345-14200 | July 17 | 19:52 | 39,000 | —51 | 8500 | 4-1 |
|  | b* | 13410-14200 | July 17 | 19:39 | 39,000 | —51 | 8500 | 4-1 |
|  | c* | 14200-15033 | July 17 | 19:55 | 39,000 | —51 | 8500 | 4-1 |
|  | d* | 14200-15033 | July 17 | 19:43 | 39,000 | —51 | 8500 | 4-1 |
| 2 | B11 a* | 15033-15850 | July 17 | 19:58 | 39,000 | —51 | 8500 | 4-1 |
|  | b* | 15033-15850 | July 17 | 19:46 | 39,000 | —51 | 8500 | 4-1 |
|  | c* | 15850-16664 | July 17 | 20:01 | 39,000 | —52 | 8500 | 4-1 |
|  | d* | 15850-16664 | July 17 | 19:48,20:06 | 39,000 | —51, —52 | 8500 | 4-1, -1, -2 |
| 3 | B12 a* | 16664-17483 | July 17 | 20:09 | 39,000 | —52 | 8500 | 4-2 |
|  | b* | 16664-17483 | July 17 | 20:26 | 36,500 | —52 | 8500 | 4-2 |
|  | c* | 17483-18282 | July 17 | 20:30 | 35,000 | —50 | 8500 | 4-2 |
|  | d* | 17483-18282 | July 17 | 20:12 | 39,000 | —52 | 8500 | 4-2 |
| 4 | B13 a* | 18282-19070 | July 17 | 20:16 | 39,000 | —52 | 8500 | 4-2 |
|  | b* | 18282-19070 | July 17 | 20:33 | 35,000 | —50 | 8500 | 4-2 |
|  | c | 19070-19800 | July 15 | 20:15 | 40,000 | —54 | 8000 | 4-4 |
|  | d | 19070-19800 | July 15 | 19:59 | 40,000 | —54 | 8000 | 4-4 |
| 5 | B14 a | 19800-20529 | July 15 | 20:18 | 40,000 | —54 | 8000 | 4-4 |
|  | c | 20529-21250 | July 15 | 20:32 | 40,000 | —54 | 8000 | 4-4 |
|  | d | 20529-21250 | July 15 | 20:06 | 40,000 | —54 | 8000 | 4-4 |
| 6 | B15 a | 21250-21986 | July 17 | 18:25 | 39,000 | —49 | 8500 | 4-1 |
|  | b | 21250-21986 | July 17 | 18:20 | 39,000 | —49 | 8500 | 4-1 |
|  | c | 21986-22660 | July 17 | 18:29 | 39,000 | —49 | 8500 | 4-1 |
|  | d | 21986-22660 | July 15 | 20:39 | 40,000 | —54 | 8000 | 4-5 |
| 7 | B16 a | 22660-23345 | July 17 | 18:31,18:37 | 39,000 | —49 | 8500 | 4-1 |
|  | b | 22660-23345 | July 15 | 20:42 | 40,000 | —45 | 8000 | 4-5 |
|  | c | 23345-24006 | July 17 | 18:52 | 39,000 | —49 | 8500 | 4-2 |
|  | d | 23345-24006 | July 17 | 18:41 | 39,000 | —49 | 8500 | 4-1, 4-2 |
| 8 | B17 a | 24006-24645 | July 17 | 18:44 | 39,000 | —49 | 8500 | 4-2 |
|  | b | 24006-24645 | July 17 | 18:55 | 39,000 | —49 | 8500 | 4-2, 4-3 |
|  | c | 24645-25270 | July 17 | 18:58 | 39,000 | —50 | 8500 | 4-3 |
|  | d | 24645-25270 | July 17, 18 | 18:47,19:09 | 39,000 | —49, —56 | 8500 | 4-2, 4-3 |
| 9 | B18 a | 25270-25873 | July 18 | 19:02 | 39,000 | —56 | 8500 | 4-3, 4-4 |
|  | b | 25270-25873 | July 18 | 19:11 | 39,000 | —56 | 8500 | 4-3, 4-4 |
|  | c | 25873-26440 | July 18 | 19:05 | 39,000 | —56 | 8500 | 4-4 |
|  | d | 25873-26440 | July 15 | 19:15 | 40,000 | —50 | 8000 | 5-4 |
| 10 | B19 a | 26440-26965 | July 18 | 19:26 | 39,000 | —56 | 8500 | 5-5 |
|  | b | 26440-26965 | July 15 | 19:17,19:21 | 40,000 | —50 | 8000 | 5-4, -5, -6 |
|  | c | 26965-27461 | July 15 | 19:23 | 40,000 | —51 | 8000 | 5-6 |
|  | d | 26965-27461 | July 18 | 19:29 | 39,000 | —56 | 8500 | 5-5 |
| 11 | B20 a | 27461-27990 | July 15 | 19:25,19:39 | 40,000 | —51, —52 | 8000 | 5-6, 5-5 |
|  | b | 27461-27990 | July 15 | 19:29 | 40,000 | —52 | 8000 | 6-2 |
|  | c | 27990-28498 | July 15 | 19:42,19:54 | 40,000 | —53 | 8000 | 5-5, -5, -6 |
|  | d | 27990-28498 | July 15 | 19:31,19:09 | 40,000 | —52, —50 | 8000 | 6-2, 5-5 |
| 12 | B21 a | 28498-28980 | July 15 | 19:56 | 40,000 | —53 | 8000 | 5-6 |
|  | b † | 28980-30705 | July 19 | 19:42 | 39,000 | —52 | 8500 | 6-2 |
|  | c † | 30705-32430 | July 19 | 19:45 | 39,000 | —52 | 8500 | 6-2, 6-3 |
|  | d † | 32430-34100 | July 19 | 19:48 | 39,000 | —52 | 8500 | 6-3 |

\* 1 μ filter. † 4 μ grating (300 1/mm), 2.4 μ filter, slit 0.30 mm, $\tau = 0.6$ sec.

⊙

*Fig. 1*  B-spectrometer record of solar spectrum λλ 13345-15033.
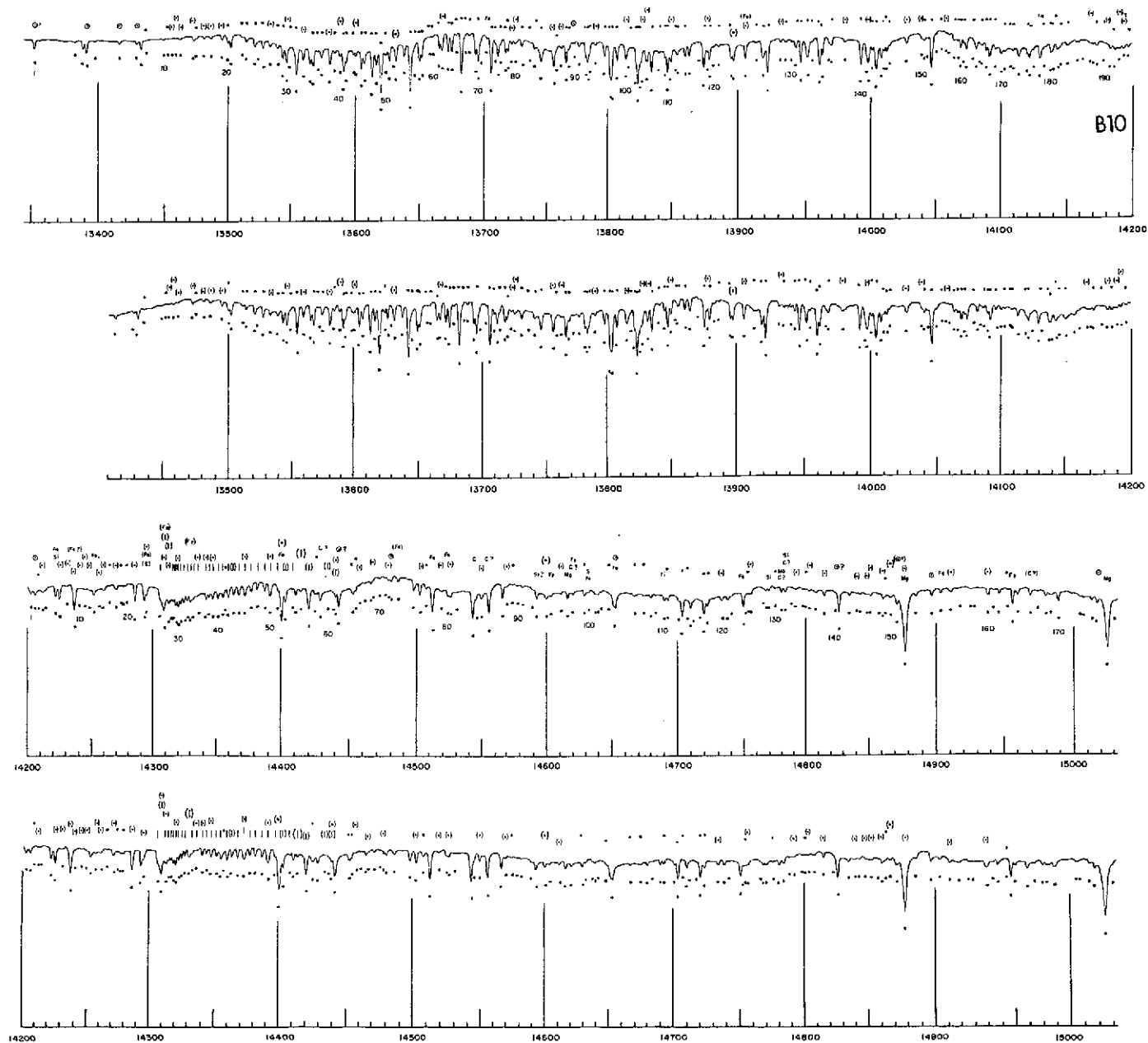
*Fig. 2*    B-spectrometer record of solar spectrum λλ 15033-16664.
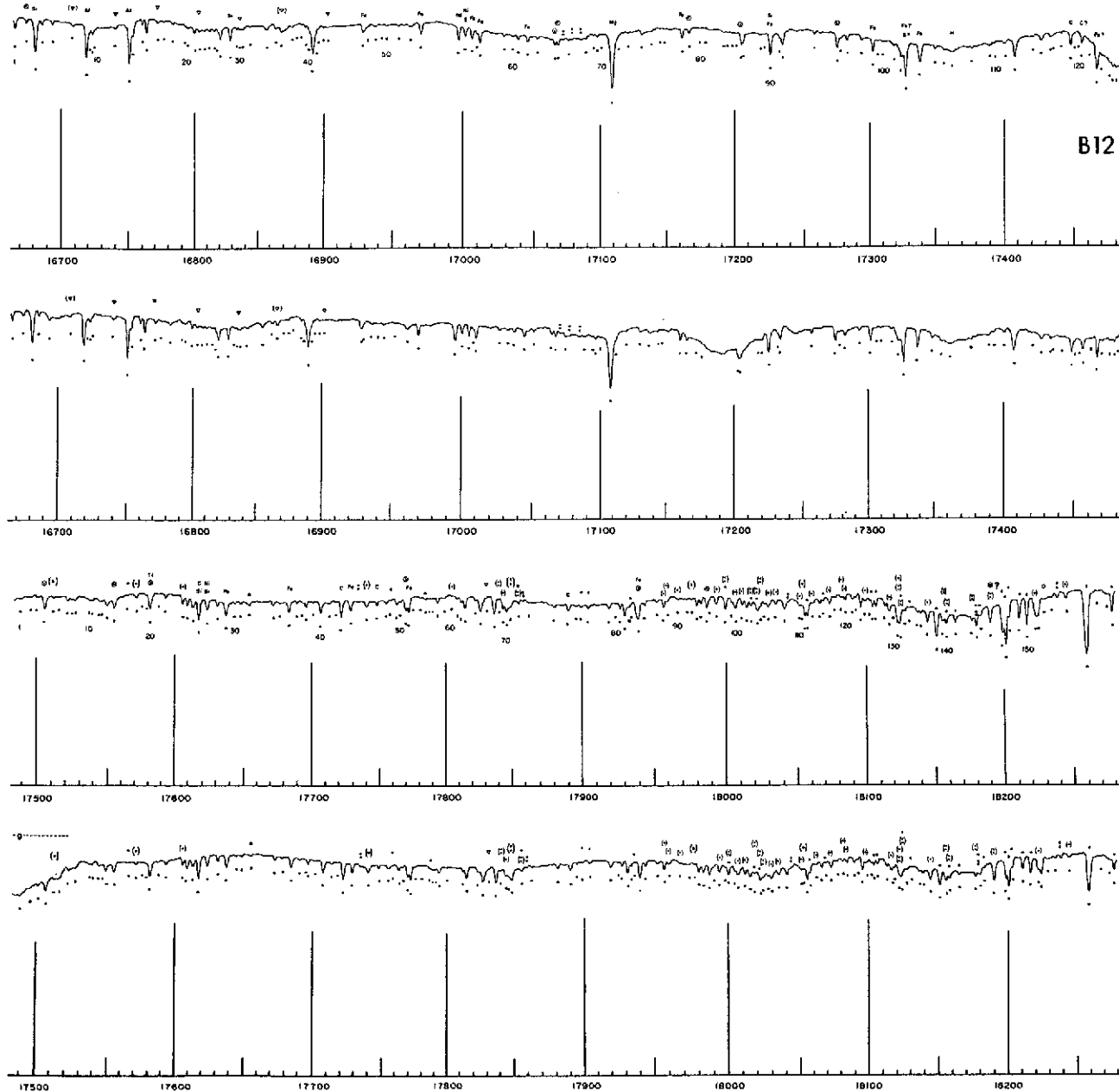
*Fig. 3* B-spectrometer record of solar spectrum λλ 16664-18282.

*Fig. 4* B-spectrometer record of solar spectrum λλ 18282-19800.

D. C. Benner, G. P. Kuiper, L. Randic and A. B. Thomson
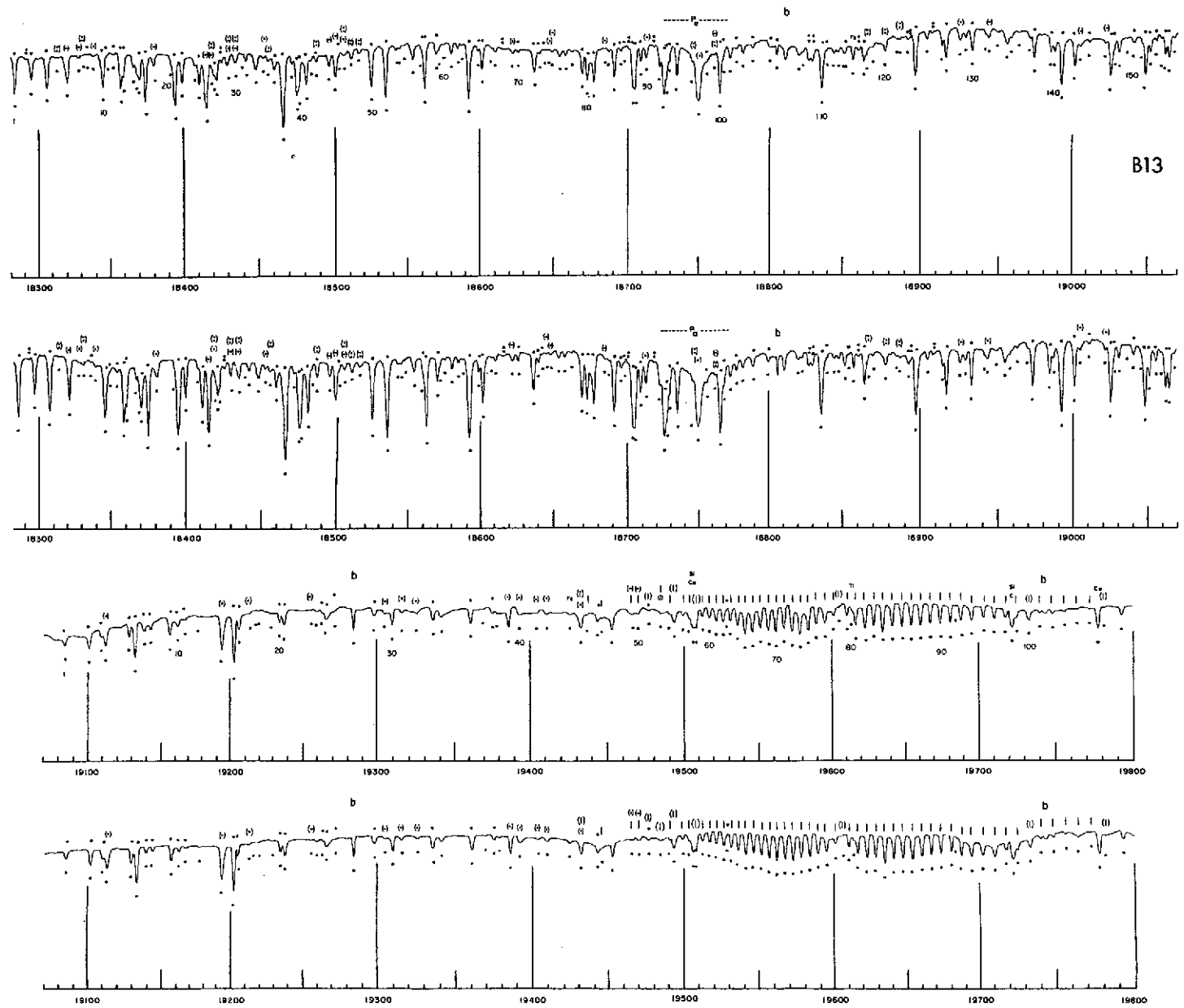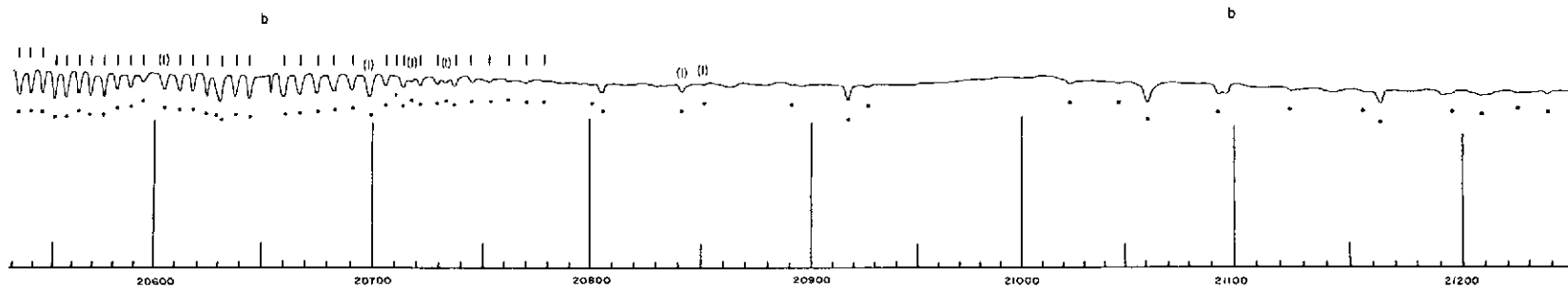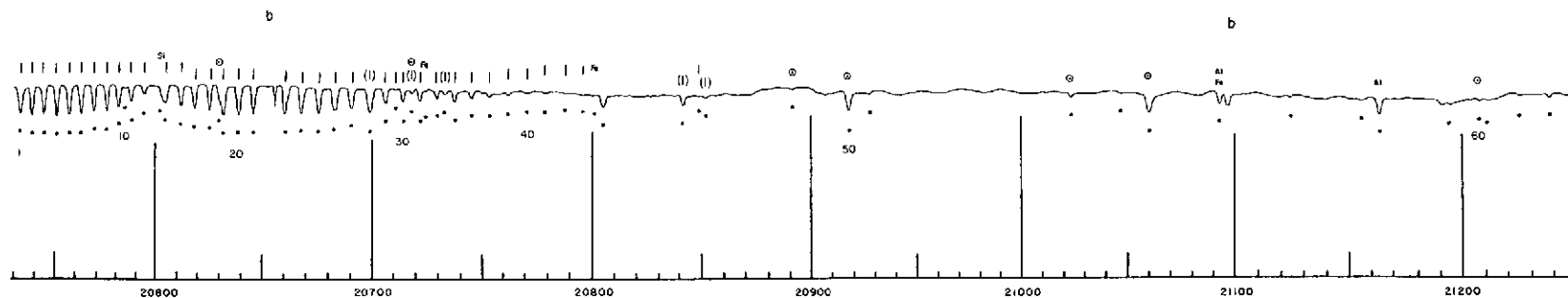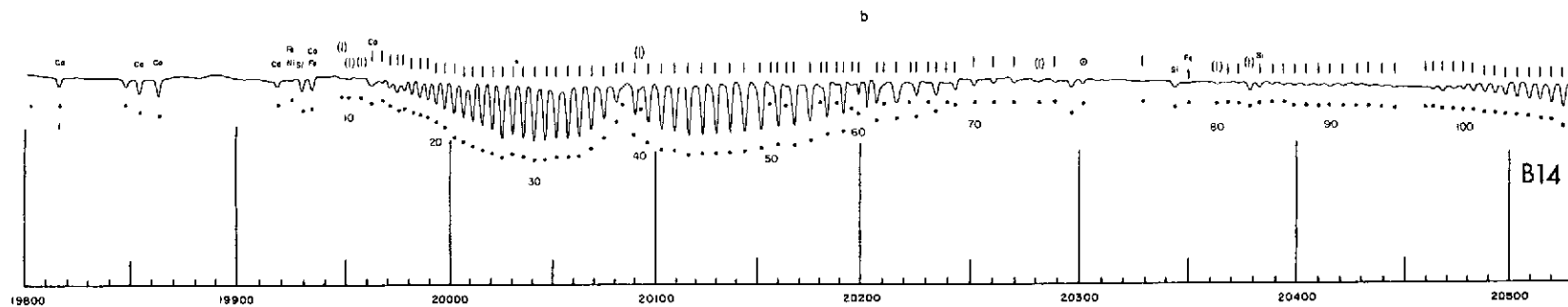


*Fig. 5*   B-spectrometer record of solar spectrum λλ 19800-21250.
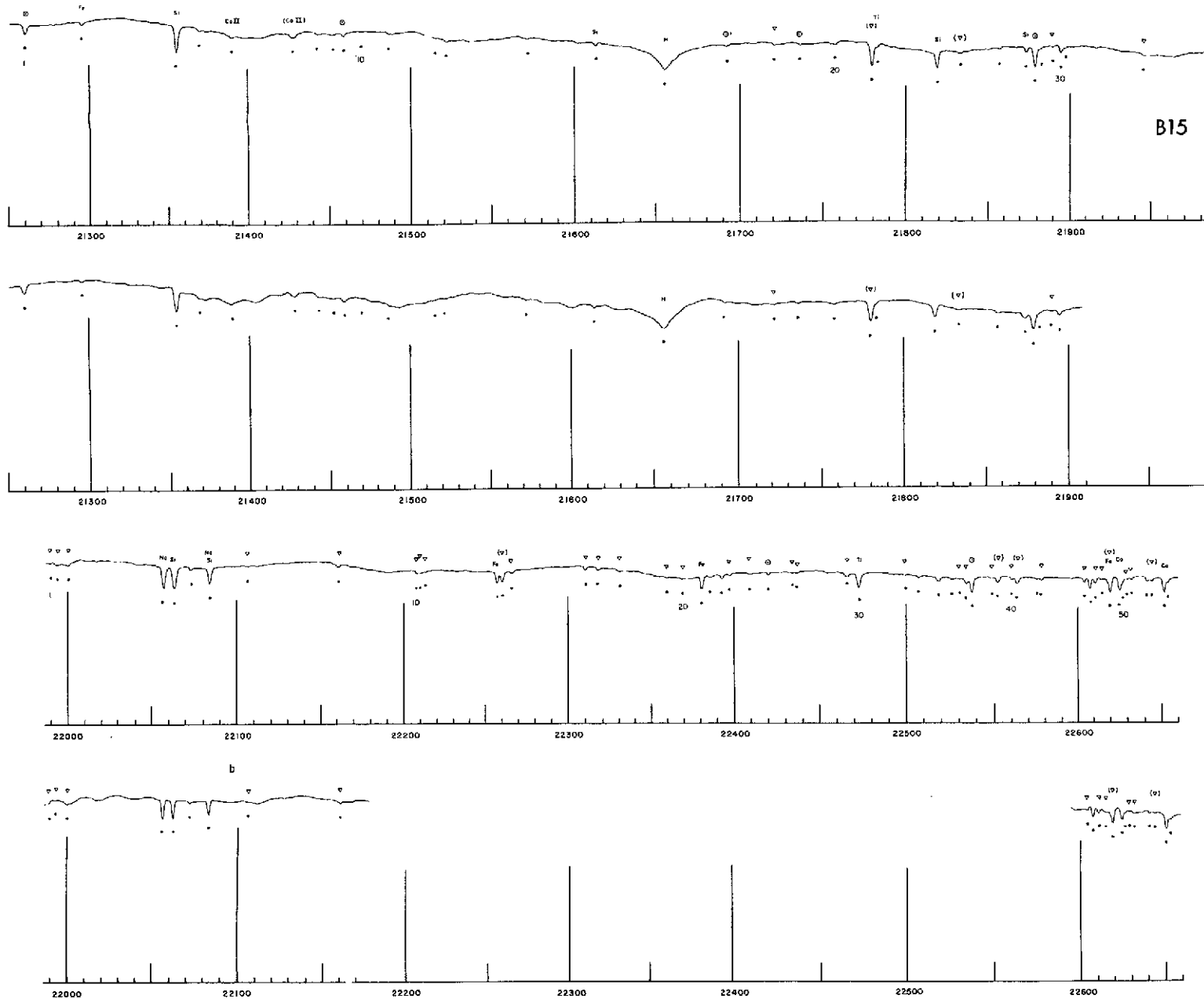
*Fig. 6*   B-spectrometer record of solar spectrum λλ 21250-22660.
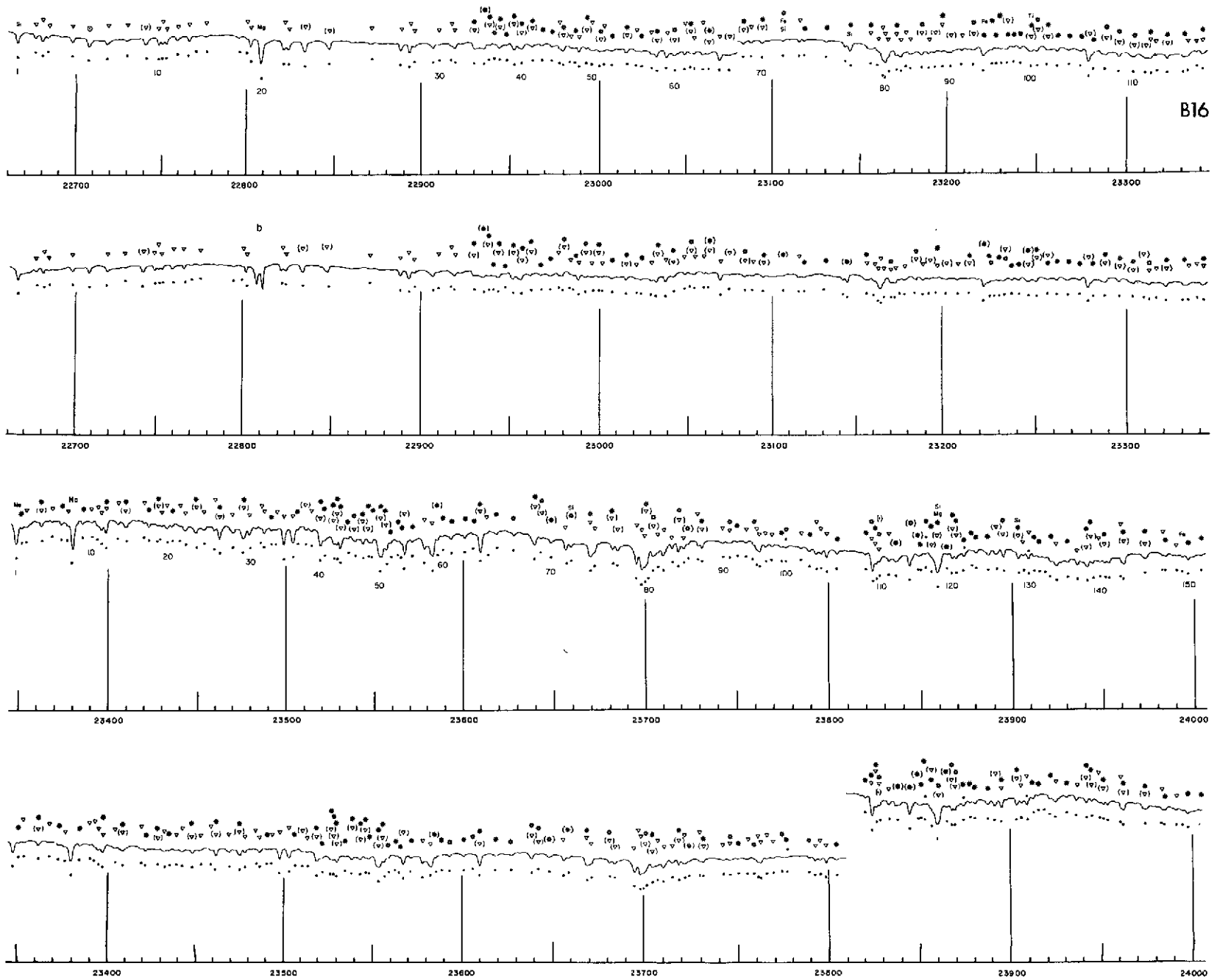
*Fig. 7* B-spectrometer record of solar spectrum λλ 22660-24006.
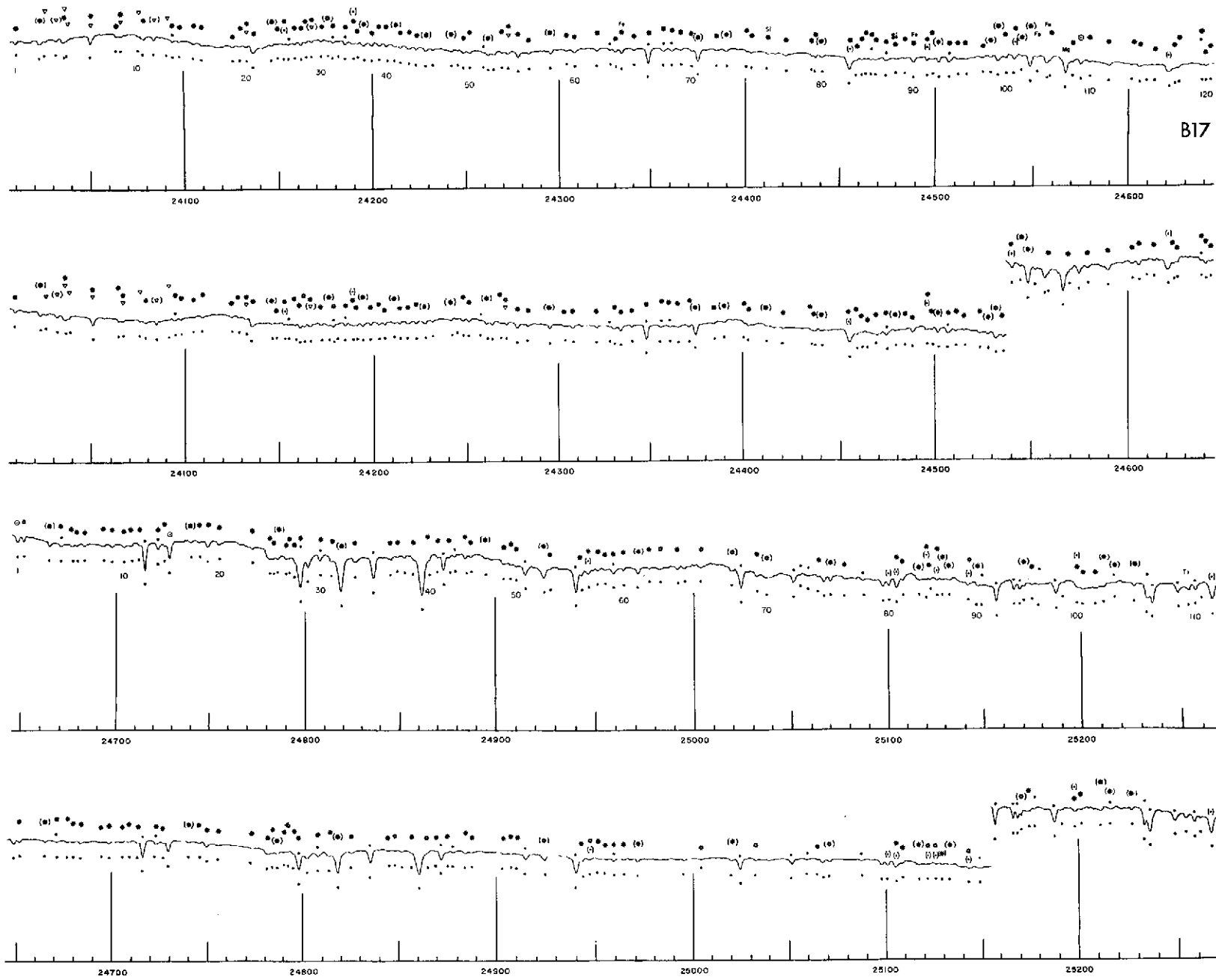
*Fig. 8*  B-spectrometer record of solar spectrum λλ 24006-25270.
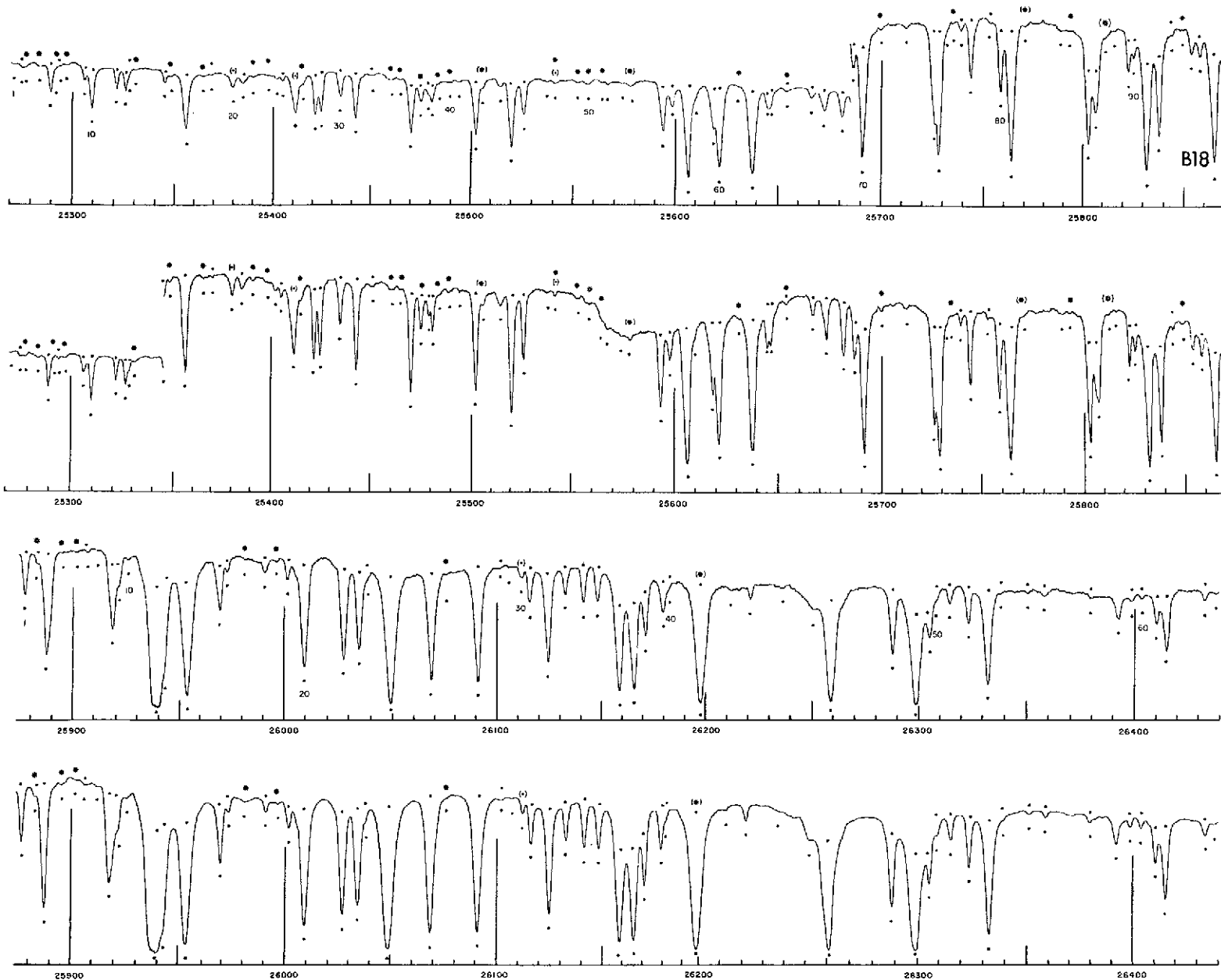
*Fig. 9* B-spectrometer record of solar spectrum λλ 25270-26440.

*Fig. 10* B-spectrometer record of solar spectrum λλ 26440-27461.

D. C. BENNER, G. P. KUIPER, L. RANDIĆ AND A. B. THOMSON
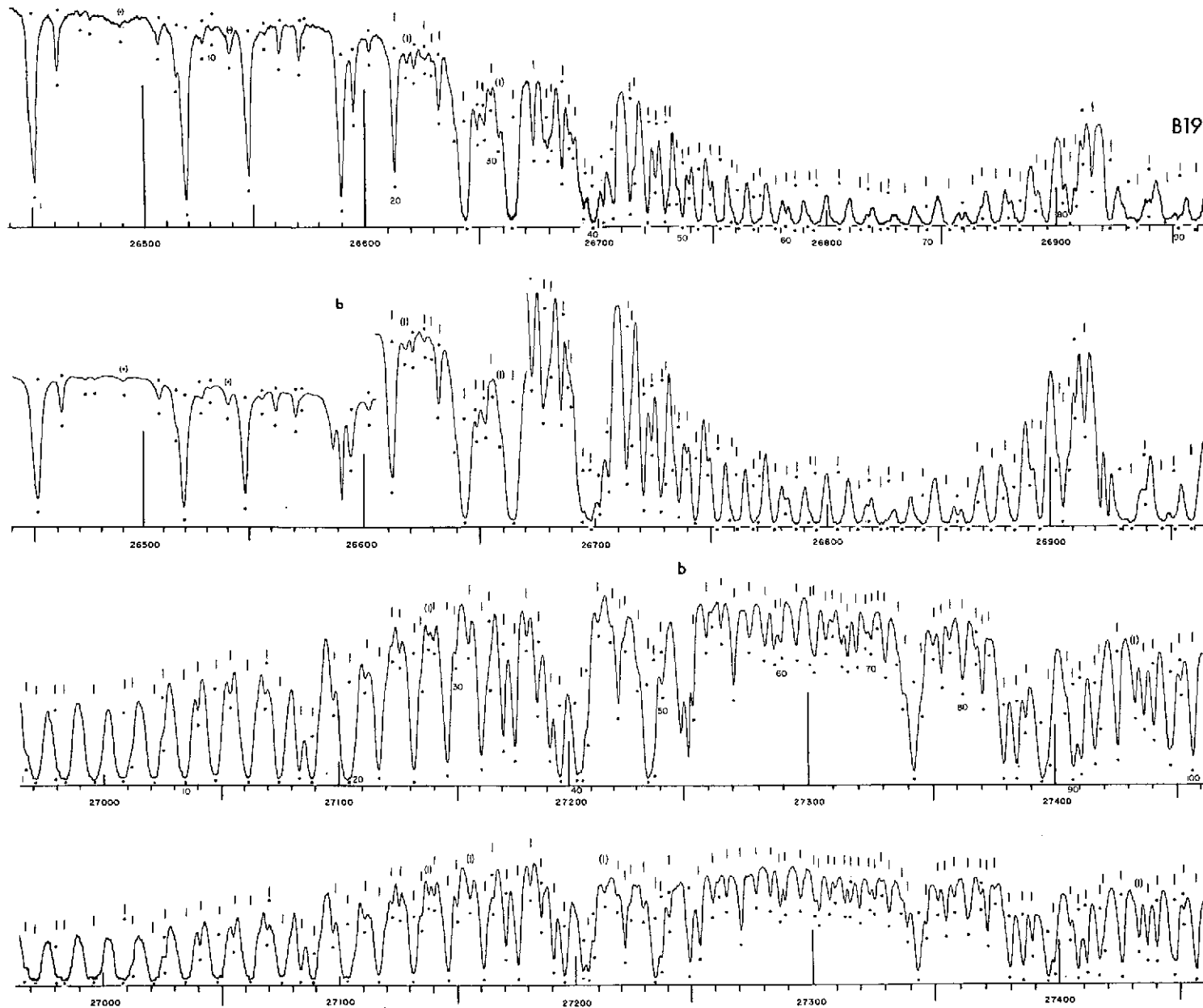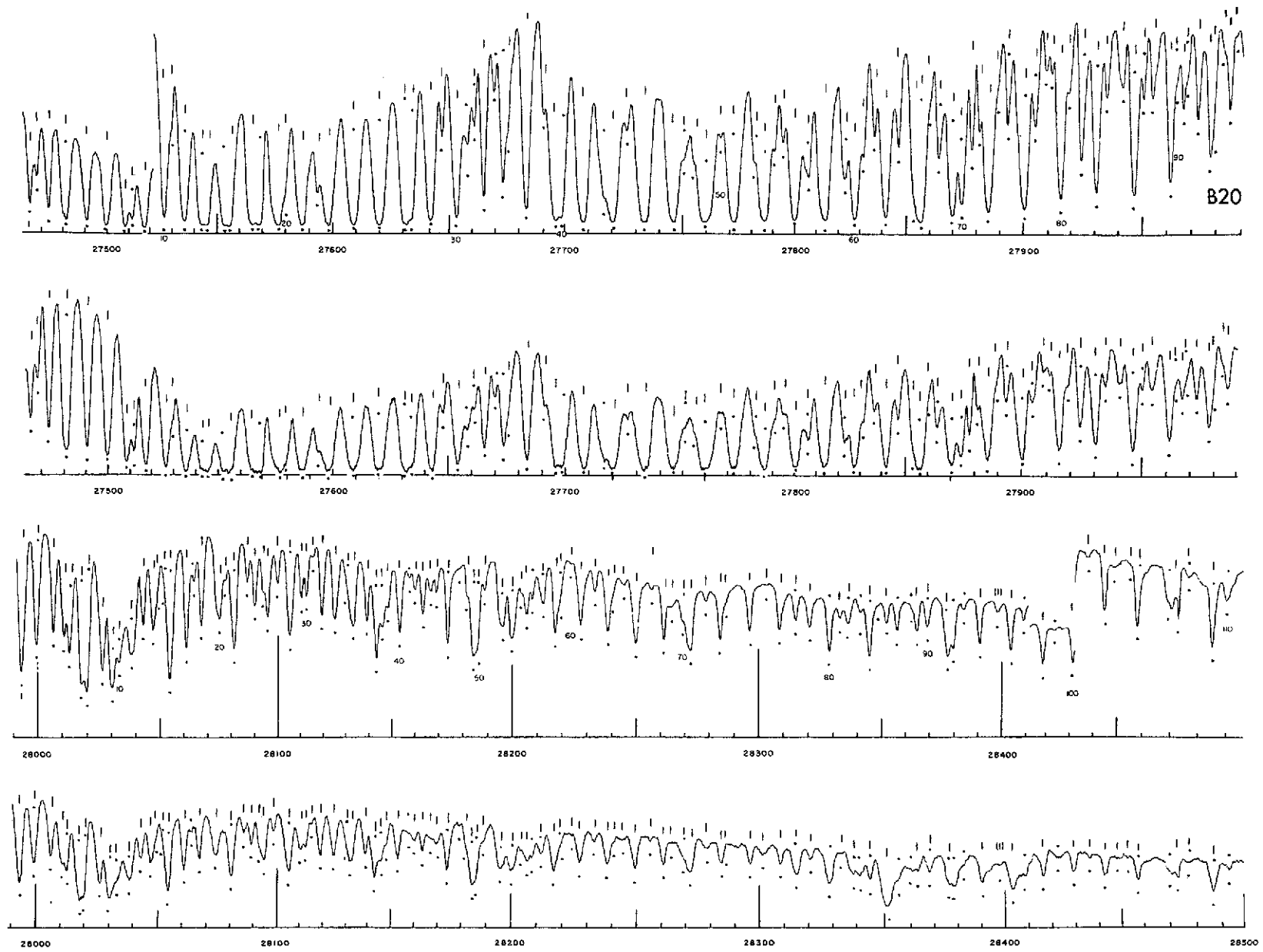
*Fig. 11* B-spectrometer record of solar spectrum λλ 27461-28498.
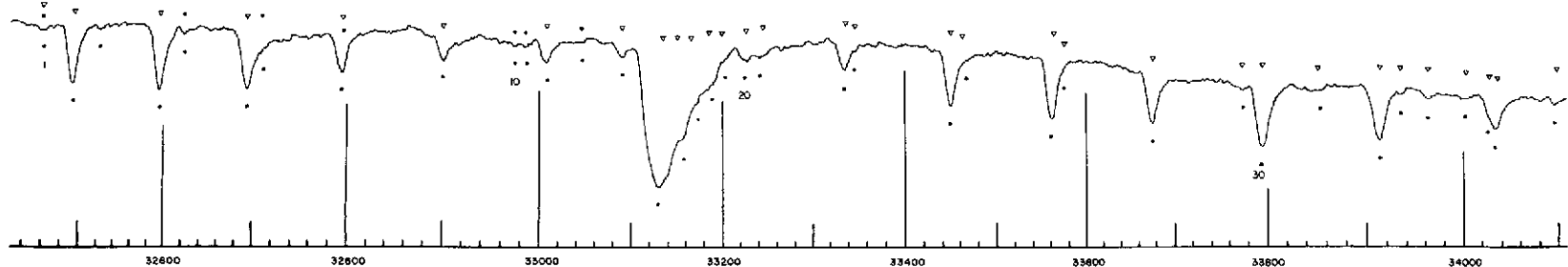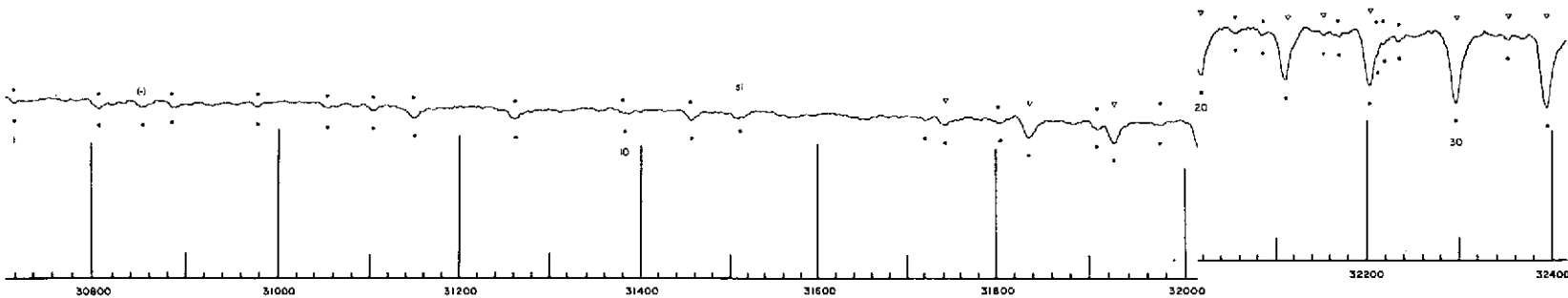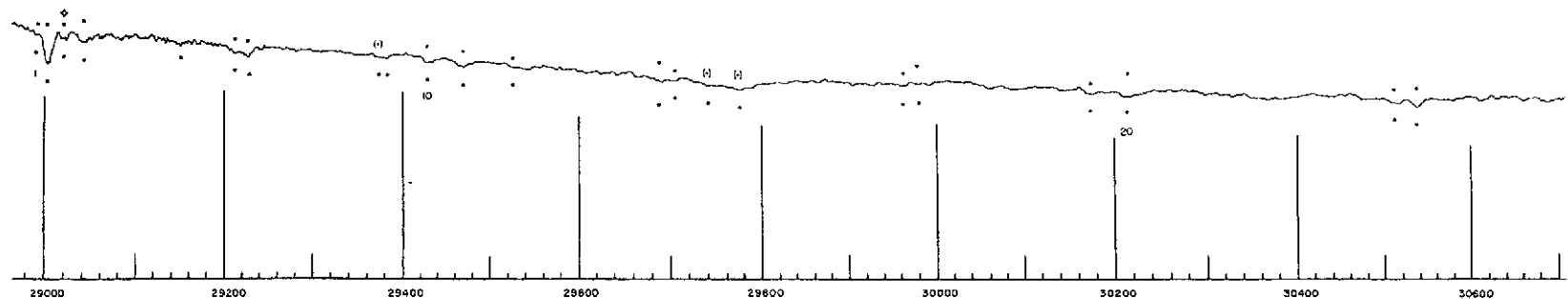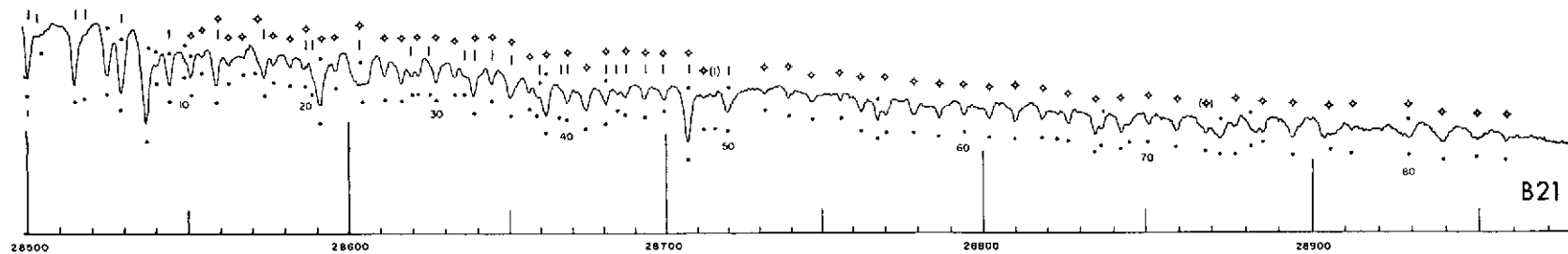
*Fig. 12*  B-spectrometer record of solar spectrum λλ 28498-34100.

# No. 167 NARROW-BAND PHOTOMETRY OF THE GALILEAN SATELLITES

*by* WILLEM WAMSTEKER

May 30, 1972

## ABSTRACT

Observations were made of the Galilean satellites in a narrow-band photometric system with a resolution of ~30 that covers the wavelength range from $0.3-1.1\mu$. The absolute scale of the system is determined from stellar model computations. It is concluded that 35 Leo, the main comparison star used, has an energy distribution similar to the sun. An attempt is made to interpret the albedo curves in terms of surface constituents.

## 1. Instrumentation

This paper is an attempt to use low-resolution spectrometry in the study of the surfaces of the Jovian satellites. This method was, among others, used successfully by McCord *et al.* (1970) on the asteroid Vesta, which led to the identification of pyroxene.

The Laboratory had acquired a set of 42 narrow-band interference filters from Infrared Industries, Thin Film Products Division, 62 Fourth Avenue, Waltham, Massachusetts. The bandwidth of the filters had been selected to represent a constant resolution of $\lambda/\triangle\lambda \sim 30$ over the full wavelength range

$0.3-1.1\mu$. The filters are mounted in three separate wheels each containing 14 filters, with the last filter repeated in the next set. The filter wheels were adapted to a single-channel photometer of the standard Johnson type (Johnson and Mitchell 1962).

An S-20 cathode was used for $0.30-0.72\mu$ and an S-1 for $0.72-1.1\mu$. The observations were made with the 61- and 40-inch telescopes of the Catalina Observatory, around the 1971 opposition of Jupiter. Owing to the low declination of Jupiter and the unfavorable summer observing conditions, the coverage is not as extensive as was intended. However all satellite data presented are an average of at least two observations on different nights.

171

Atmospheric extinction was allowed for by average extinction coefficients derived independently, checked on some nights by the observation of stars at small and large air masses. Allowance was also made for nights with high and low humidity within the well-known atmospheric water-vapor absorptions.

Table I gives the observations as "normalized" albedos, with the maximum put at unity. The values are ratios of the satellite intensities in terms of HR 4030 (35 Leo). Wavelength regions observed at different orbital phases of the satellites were adjusted to each other by means of the filters common to both data sets. The wavelengths in the first column of Table I are those midway between the 50 percent transmission points of the filters, assuming a flat radiation source.

## 2. Comparison Stars

A number of G2V-stars were observed to obtain sources with spectra similar to the sun. However, the average solar-type star is not identical to the sun, as shown by Code (1960). To acquire an independent estimate of the similarity of the spectral distributions of sun and comparison stars, we also observed a number of stars included in the absolute stellar calibration by Hayes (1970). The disadvantage of this calibration is that it applies only to regions which are free of spectral lines. To overcome this problem, we used Mihalas' (1966) hydrogen line-blanketed models. The star which was most suited for this purpose was HR 4468 ($\theta$Crt, B9V), which is included in Hayes' calibration, has a spectral type covered by Mihalas' (log g, $\theta$)-range, and is early enough to be considered still undisturbed by metal absorptions at the resolution of our photometric system.

A first direct comparison between our photometric system and Hayes' calibration, in which the energy distributions relative to HR 4468 are taken, showed both systems to be consistent within 2 percent in regions free of lines. The spectral range covered by this comparison was from B3V to A1V. Shortward of $0.36\mu$ the deviations were somewhat larger for B3V but still did not exceed 5 percent.

The stellar model chosen for HR 4468 is specified by Mihalas with the parameters log g=4, $\theta$=0.45. To convert the model into our photometric system, the filter bandpasses were assumed to be square.

With the information from the model it is possible to construct an energy distribution for each

Table I

Normalized Relative Reflectivities of Galilean Satellites

| λ(μ) | Io | Europa | Ganymede | Callisto |
|---|---|---|---|---|
| 0.300 | 0.216 | 0.332 | 0.476 | 0.392 |
| 0.308 | 0.108 | 0.408 | 0.389 | 0.436 |
| 0.318 | 0.075 | 0.370 | 0.375 | 0.382 |
| 0.328 | 0.096 | 0.378 | 0.386 | 0.403 |
| 0.340 | 0.096 | 0.410 | 0.446 | 0.440 |
| 0.350 | 0.097 | 0.422 | 0.490 | 0.483 |
| 0.358 | 0.104 | 0.448 | 0.547 | 0.515 |
| 0.368 | 0.132 | 0.491 | 0.582 | 0.547 |
| 0.378 | 0.123 | 0.510 | 0.591 | 0.552 |
| 0.390 | 0.164 | 0.570 | 0.639 | 0.612 |
| 0.399 | 0.213 | 0.592 | 0.683 | 0.639 |
| 0.423 | 0.331 | 0.673 | 0.723 | 0.683 |
| 0.444 | 0.462 | 0.751 | 0.785 | 0.756 |
| 0.457 | 0.566 | 0.810 | 0.833 | 0.783 |
| 0.478 | 0.671 | 0.857 | 0.870 | 0.823 |
| 0.498 | 0.749 | 0.891 | 0.905 | 0.858 |
| 0.518 | 0.776 | 0.895 | 0.919 | 0.885 |
| 0.538 | 0.794 | 0.898 | 0.920 | 0.906 |
| 0.560 | 0.801 | 0.920 | 0.942 | 0.934 |
| 0.578 | 0.813 | 0.937 | 0.945 | 0.951 |
| 0.599 | 0.847 | 0.964 | 0.969 | 0.975 |
| 0.615 | 0.877 | 0.968 | 0.995 | 0.991 |
| 0.637 | 0.954 | 0.983 | 0.993 | 0.996 |
| 0.652 | 0.954 | 0.994 | 1.000 | 0.986 |
| 0.672 | 0.983 | 1.000 | 0.997 | 0.998 |
| 0.698 | 1.000 | 0.998 | 0.985 | 0.989 |
| 0.717 | 0.994 | 0.994 | 0.978 | 0.986 |
| 0.746 | 0.986 | 0.986 | 0.987 | 1.000 |
| 0.767 | 0.979 | 0.996 | 0.967 | 0.984 |
| 0.787 | 0.963 | 0.975 | 0.960 | 0.981 |
| 0.808 | 0.960 | 0.988 | 0.966 | 0.988 |
| 0.838 | 0.925 | 0.960 | 0.931 | 0.962 |
| 0.862 | 0.948 | 0.992 | 0.950 | 0.985 |
| 0.894 | 0.933 | 0.976 | 0.912 | 0.958 |
| 0.923 | 0.911 | 0.998 | 0.910 | 0.951 |
| 0.950 | 0.921 | 0.982 | 0.894 | 0.960 |
| 0.996 | 0.887 | 0.956 | 0.864 | 0.931 |
| 1.032 | 0.868 | 0.910 | 0.830 | 0.934 |
| 1.080 | 0.831 | 0.874 | 0.823 | 0.916 |
| 1.105 | 0.805 | 0.860 | 0.800 | 0.883 |

observed star. The energy distributions thus derived for a B3V star and an A1V (resp. HR 3454 and HR 4963) are from $0.45\mu$ to $0.70\mu$, similar to Hayes' calibration for the regions where the influence of the hydrogen lines is negligible. Over this region the deviations do not exceed 2 percent. Shortward of $0.36\mu$ the deviations were larger, if the energy distributions were matched over the range from $0.45\mu$ to $0.70\mu$. This, however, can easily be caused by a slight mismatch of the model parameters. This seems to be the case, because the deviations are of the same order of magnitude and sign both for the A1V star and the B3V star. Since the deviations in this case were somewhat larger than the deviations between our system and Hayes' as mentioned before, at $\lambda < 0.36\mu$ we applied a correction for this.

The corrections, which are listed in Table II, are such that the energy distribution derived by the model has to be multiplied by the correction factor to be consistent with Hayes' calibrations.

## TABLE II
Correction Factors Applied to Model-Derived
Energy Distribution

| $\lambda$ ($\mu$) | CORRECTION FACTOR |
|-------------------|-------------------|
| 0.300 | 0.88 |
| 0.308 | 0.88 |
| 0.318 | 0.88 |
| 0.328 | 1.00 |
| 0.340 | 1.05 |
| 0.350 | 1.50 |

The two shortest wavelengths listed in Table II were assumed to need the same correction factor as determined for $\lambda$=0.318$\mu$; this may not be strictly correct in view of the trend longward of 0.318$\mu$. At the long wavelength end of the spectrum there still remains the Paschen jump and the Paschen lines. However, the filter transmission bands are wider in that region ($\triangle\lambda\sim0.03\mu$). The Paschen jump, which is not very large, will tend to be smoothed out by the bandwidth and the effect of overlapping lines. For these reasons, we smoothed the energy distribution of the stellar model (log g $=$ 4, $\theta$ $=$ 0.45) through towards the longer wavelengths.

Figure 1 shows the energy distribution of HR 4030 (35 Leo) thus derived, from Mihalas' model (log g $=$ 4, $\theta =$ 0.45) and the observations of HR 4030 and HR 4468. The dotted line is the energy distribution of the sun from Labs and Neckel (1968). Although in detail there are some discrepancies, the overall agreement is very good. At the two shortest wavelengths HR 4030 seems too high, but that could be caused by the fact that the correction factor derived for 0.318 was used. The match for the other solar-type stars observed was considerably worse. These will be discussed elsewhere.
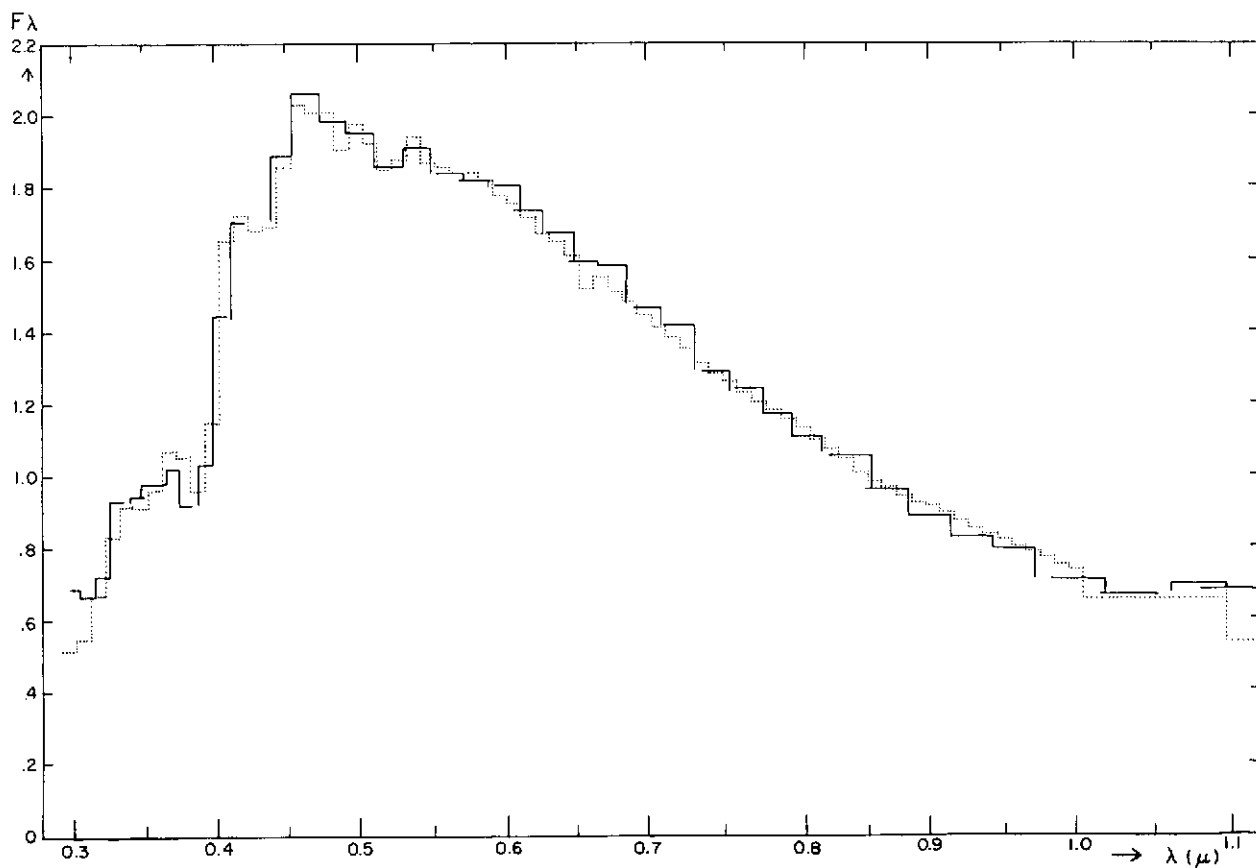


*Fig. 1.* Comparison between flux distributions of the sun (dotted line: Labs and Neckel 1968) and 35 Leo (HR 4030). Unit of $F_\lambda$ is Wcm$^{-2}\mu^{-1}$ x const.

### 3. The Albedo Curves

Figure 2 shows the albedo wavelength curves for the Galilean satellites. The left-and-right hand ordinates are respectively normalized and geometrical albedos. The geometrical albedos used here are described in Appendix 1. The error bars drawn in Figure 2 are the average deviations from the mean.

The normalized reflection curves for all four satellites look similar. They all show a decrease in the albedo towards shorter wavelengths. For Io the decrease starts around $0.7\mu$ and for the three outer ones at $\sim 0.6\mu$. From $0.6\mu$ longward the albedo curves are more or less flat with a slight decrease at the longest wavelengths. Apart from a shallow absorption feature between $0.5\mu$ and $0.6\mu$, the
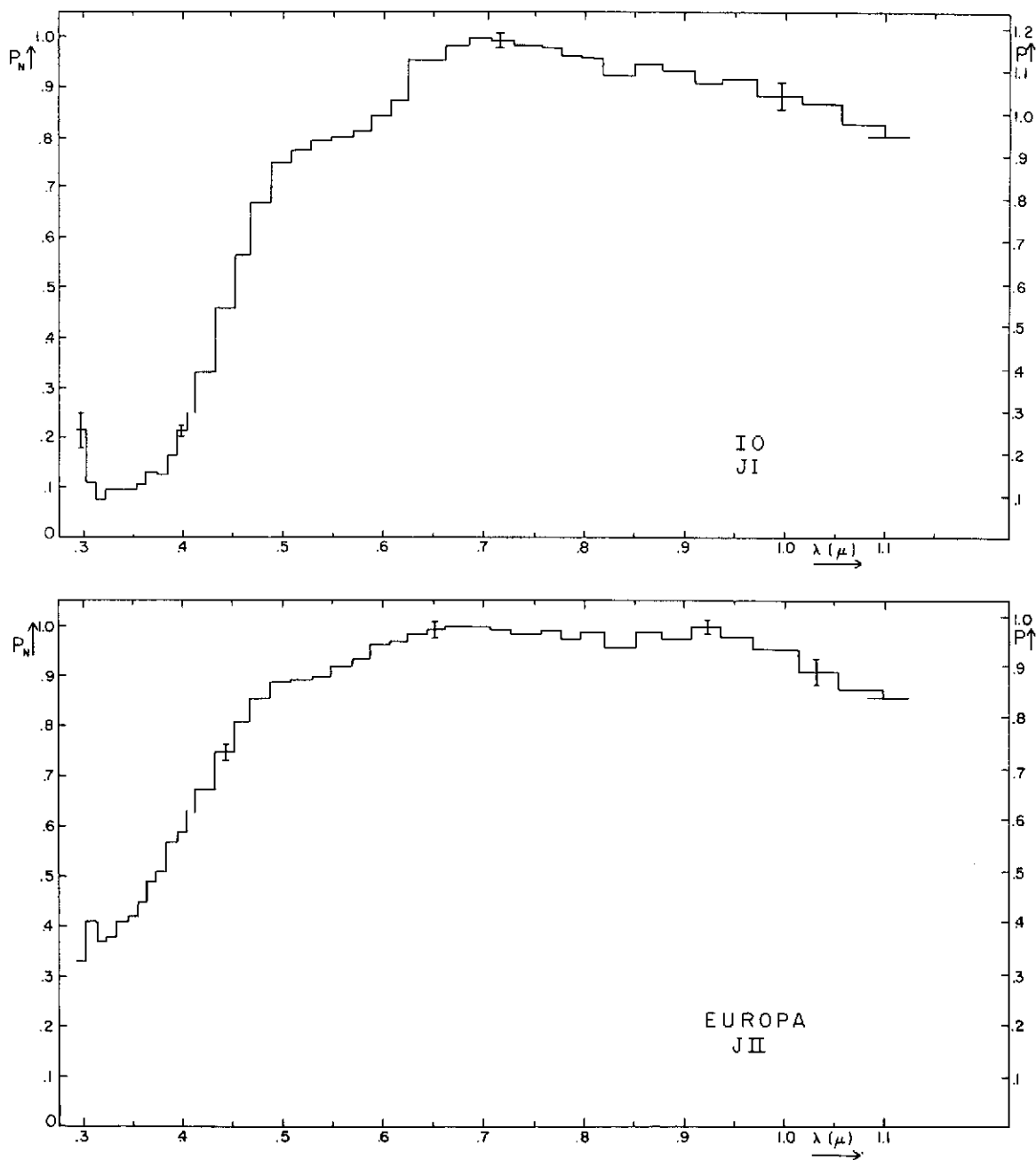


*Fig. 2* Wavelength dependence of geometrical albedos of Galilean satellites; normalized albedos, $P_n$ at left; geometrical albedos, P, derived in Appendix I, at right. Representative error bars show average deviations from the mean.

albedo curves are without any distinct features. This shallow feature is not present in the curve for J IV.

The curves are similar to the albedo-wavelength dependence found by Johnson (1971), but not identical. In the present data the absorption feature at $\lambda \sim 0.55\mu$ shown by Johnson for Io seems to be present also in the reflectivity curves for Europa and Ganymede, although less pronounced. Further,

Johnson's data show a stronger decrease in albedo longward of $0.95\mu$.

The similarity between the four satellites in the albedo-wavelength dependence exists only in the "normalized" curves. If one considers the geometrical albedos, a quite different picture emerges. In fact, the right-hand ordinates of Figure 2 show that the satellite albedos differ by a factor of 4.
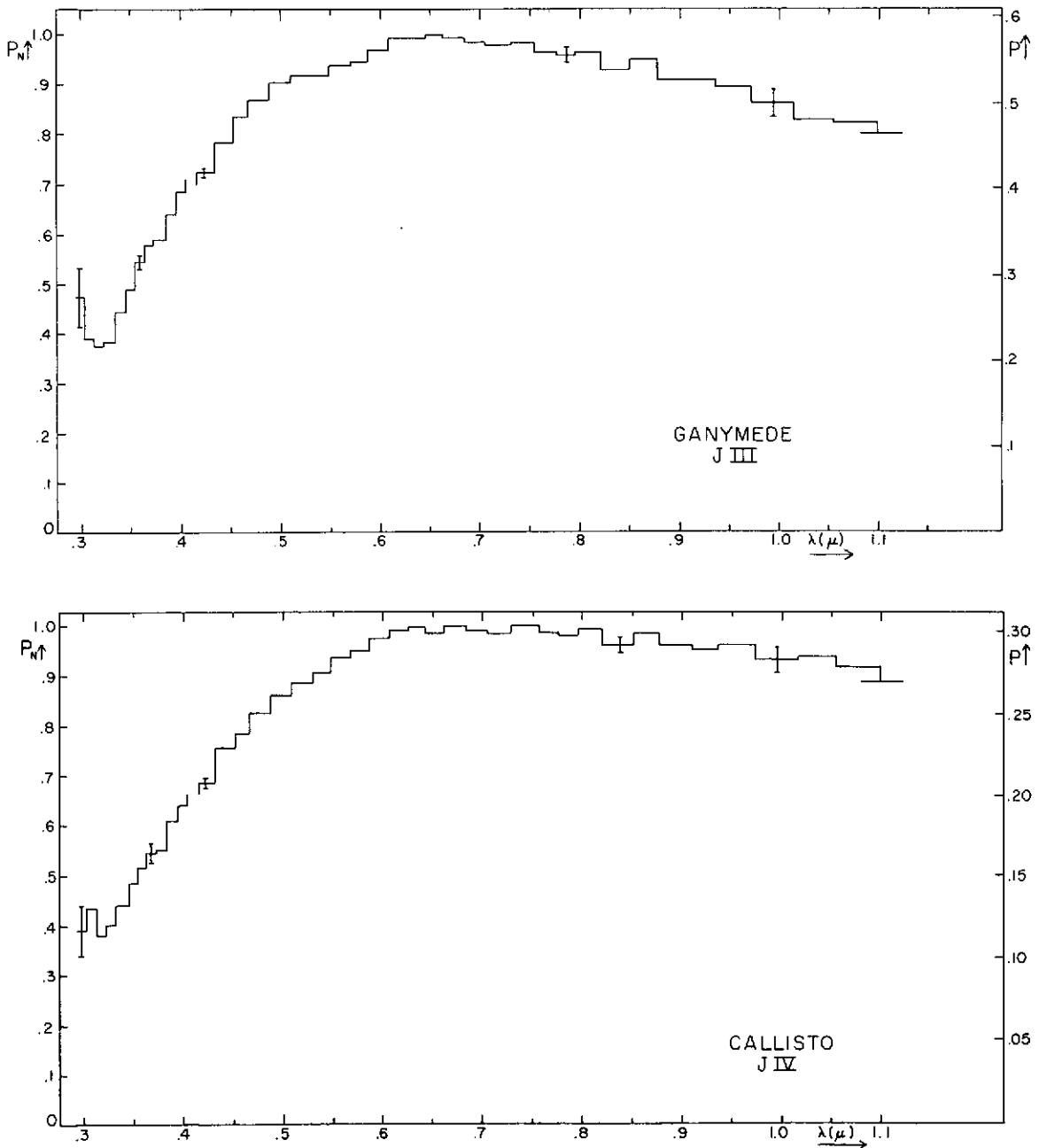


Fig. 2, continued.

Table III gives the highest and lowest albedos measured for each satellite, together with the wavelengths at which they occur.

TABLE III

Maximum and Minimum Albedos of Galilean Satellites
$(0.3\mu < \lambda < 1.1\mu)$

|  | $\lambda$ MAX | P MAX | $\lambda$ MIN | P MIN |
|---|---|---|---|---|
| J I | 0.70 | 1.18 | 0.32 | 0.09 |
| J II | 0.67 | 0.98 | 0.30 | 0.32 |
| J III | 0.65 | 0.58 | 0.32 | 0.22 |
| J IV | 0.75 | 0.30 | 0.32 | 0.12 |

Table III further indicates that, although the "normalized" albedo curves are similar in appearance, this does not imply similar surface materials, unless one assumes for each satellite an appropriate amount of a featureless greying agent. The high geometrical albedos make this assumption dubious. Also, the broad-band infrared data of Lee (1972) show dissimilarities between the satellites. The absence of distinct absorption features between $0.5\mu$ and $1.1\mu$ suggests the following possibilities (Adams 1968):

(a) The absence of iron-bearing minerals.

(b) Very small particles ($<10\mu$) which reduce absorption because of reduced penetration.

(c) The presence of substantial amounts of a highly absorbing material.

In view of the high albedos for JI, JII and JIII possibility (c) is improbable for them. The weakening of the absorptions by very small particles might be present. The absence of iron-bearing minerals seems confirmed. The most conspicuous common spectral feature of the satellites is the nearly uniform drop in reflectivity from $0.5-0.3\mu$. This has not been explained. Sulfur and some of its compounds exhibit this property, but its common presence on other solar-system bodies (the Moon, Mercury, Saturn's Rings) suggest other possibilities, such as radiation damage.

In the following we will see what additional conclusions can be drawn from the albedo wavelength dependence from $0.3\mu$ to $1.1\mu$. We will also make use of the broad-band infrared data in the Johnson JHKL-system (Lee, *op. cit.*)

### 4. Io

The strong UV absorption appears to rule out a cover by ice. Although various substances studied by Sill (Sill 1972 and Kuiper 1969) show UV absorptions, most of these are not very strong. Of the more abundant substances only sulfur and some of its compounds match the general run of the Io

albedo curve. While some other compounds also show fairly strong UV absorptions, they are less probable on grounds of abundance. Now the slope of the UV sulfur absorption is dependent on the specific compounds; and, as is shown by Sill (1972), the position and slope of the ultraviolet absorption are temperature-dependent. The reflectivity of sulfur compounds increases with decreasing temperature, which might explain the high albedo of Io. Sill's reflection curves of ammonia compounds show a number of absorptions which are not seen in the albedo-wavelength dependence of Io. $NH_4 \cdot HS$ gives rise to absorptions centered at $\sim 0.6\mu$, $\sim 1.4\mu$, $\sim 1.7\mu$ and $\sim 2.3\mu$. The narrow-band data do show an absorption at $\sim 0.55\mu$ close to the $0.6\mu$ absorption. However, the absorptions at $\lambda > 1.1\mu$ are of such strength and position that they would give rise to noticeable decrease in the observed albedo even in the broad-band data. The IR data of Lee do not show any depression. Thus there is no evidence for the presence of $NH_4 \cdot HS$, but S may be present.

### 5. Europa

The maximum albedo of JII is somewhat lower than that of Io, but still high. However, the UV absorption is considerably less strong. An absorption around $0.5\mu$ seems to be present but is not very strong. The strength of the UV absorption of Europa is such that there exists a large range of compositional possibilities. Although the ferrous ion in most samples studied by Sill shows a UV absorption of the same order of magnitude as JII, most ferrous compounds show a low albedo. However, there exists observational evidence that Europa has polar caps (Veverka 1970). The region $\lambda > 1\mu$ must be consulted for additional clues. Lee's IR data suggest a close similarity between JII and JIII.

### 6. Ganymede and Callisto

The normalized albedos of these two satellites are very similar from $0.32\mu$ to $0.92\mu$. With the observations having an accuracy of 2 percent, the ratio $p(JIII)/p(JIV)$ is found constant within the expected error limits.

However, both the absolute visual and the IR albedos are considerably different. Lee finds that the IR albedo of JIII is compatible with $H_2O$ ice. If one makes a detailed comparison between the reflection spectrum of $H_2O$ ice at $-190°$ C (Kuiper *et al.*), the agreement is very good. The probable presence of $H_2O$ on Europa and Ganymede was discovered by Kuiper (1957).

## APPENDIX I

### The Geometrical Albedo of The Galilean Satellites

Table IV lists the values of the geometrical albedos of the Jovian satellites at $\lambda_{eff.}=0.55\mu$, as derived from both narrow- and broad-band observations. For the $M_V$ of the sun we used Johnson's (1965) value of $-27.64$. The radii used are from Kuiper (1952). A change in radius of $\Delta R$ will change the albedo with a factor $(1+\Delta R/R)^2$. It is obvious from Table IV that the observational accuracy is fairly high. The main uncertainty in these numbers is still caused by the difficulty in measuring the diameter of the satellites. In determining the average value of the albedos, the measurement of Io by Lee is not taken into account. For the three other satellites all four data sets are used. The relative accuracy of the observed geometrical albedo thus derived is 3 percent (m.e.).

### TABLE IV

Geometric Albedos of the Galilean Satellites at $\lambda = 0.55\ \mu$

| | 1)<br>Radius<br>(Km.) | 2)<br>Harris | 3)<br>Lee | 4)<br>Johnson | This<br>Paper | Average |
|---|---|---|---|---|---|---|
| Io | 1625 | 0.97 | (0.73) | 0.91 | 0.94 | 0.94 |
| Europa | 1440 | 0.89 | 0.93 | 0.92 | 0.83 | 0.89 |
| Ganymede | 2510 | 0.52 | 0.51 | 0.57 | 0.54 | 0.54 |
| Callisto | 2230 | 0.27 | 0.27 | 0.30 | 0.27 | 0.28 |

1) Kuiper (1952); 2) Harris (1961); 3) Lee (1972); 4) Johnson and McCord (1970).

## REFERENCES

Adams, J. B. 1968, *Science*, 159, 1453.

Code, A. D. 1960, *Stars and Stellar Systems*, Vol. VI, ed. J. L. Greenstein (Chicago: University of Chicago Press), p. 50.

Duke, M. B., Woo, C. C., Bird, M. L., Sellen, G. A., Finkelman, R. B. 1970, *Science*, 167, 648.

Harris, D. L. 1961, *Planets and Satellites*, eds. G. P. Kuiper and B. M. Middlehurst (Chicago: University of Chicago Press), p. 272.

Hayes, D. S. 1970, *Ap. J.*, 159, 165.

Johnson, H. L., Mitchell, R. I. 1962, *LPL Comm. No. 14*, 1, 73.

Johnson, H. L. 1965, *LPL Comm. No. 53*, 3, 73.

Johnson, T. V., McCord, T. B. 1970, *Icarus*, 13, 37.

Johnson, T. V. 1971, *Icarus*, 14, 94.

Kuiper, G. P. 1952, *The Atmospheres of the Earth and Planets*, ed. G. P. Kuiper (Chicago: University of Chicago Press), p. 306.

Kuiper, G. P. 1957, *Astron. J.*, 62, 245.

Kuiper, G. P. 1969, *LPL Comm. No. 101*, 6, 229.

Kuiper, G. P., Cruikshank, D. P., Fink, U. 1970, *Sky and Telescope*, 39, 80.

Labs, D., Neckel H. 1968, *Zeitschrift für Astrophys.*, 69, 1.

Lee, T. A. 1972, *LPL Comm. No. 168*, 9, in press.

McCord, T. B., Adams, T. B., Johnson, T. V. 1970, *Science*, 168, 1445.

Mihalas, D. 1966, *Ap. J.*, Supplement Series, 13, 1.

Sill, G. 1972, "Laboratory Spectra of Selected Solids," *LPL Comm.*, in press.

Veverka, J. F. 1970, "Photometric and Polarimetric Studies of Minor Planets and Satellites," Harvard Thesis.

# No. 168 SPECTRAL ALBEDOS OF THE GALILEAN SATELLITES

## by THOMAS LEE

July 21, 1971

## ABSTRACT

The wavelength dependence of the albedo of the Galilean satellites has been determined from wide-band photometric observations extending from $0.36\mu$ to $3.4$ $\mu$.

The author has observed Jupiter's Galilean satellites with two telescopes: the 60-inch on Site II, Catalina Observatory (el. 8450 ft = 2580 m); and the 40-inch on Site IV (el. 8580 ft = 2620 m). Two standard photometers were used, one for UBVRI (with two photomultipliers, a 1P21 and a RCA 7102); and one for JHKL, using a liquid $N_2$-cooled PbS cell. The data are summarized in Table I. This table gives the photometric band designation, the effective wavelength, and the mean observed magnitude for each satellite. In all cases, the quoted magnitudes are means of several independent measures obtained within a few days of the 1971 opposition. Two sets of UBVRI observations were obtained on three nights and an average of 4.2 JHKL measures on six additional nights.

The scatter in the individual measures, particularly in the infrared (JHKL), is larger than found for routine stellar observations; e.g., the spread is $0\overset{m}{.}2$ to $0\overset{m}{.}3$ in the K magnitude. The satellites are known to vary in the visual region (Harris 1961); our observations suggest that in the infrared the variations may be somewhat larger and may be correlated with orbital phase. Because of the number of measures obtained, the average JHKL magnitudes given in Table I should be good to better than $\pm0\overset{m}{.}10$ (mean error). At shorter wavelengths, the errors will be smaller.

The observations were analyzed to determine the wavelength dependence of the albedo of these objects. The computed albedos, shown in Figure 1, are normalized to 0.5 in the visual band at $0.55\mu$.

179

TABLE I

MAGNITUDES OF GALILEAN SATELLITES

| DESIGNATION EFFECTIVE $\lambda$ ($\mu$) | U 0.36 | B 0.44 | V 0.55 | R 0.70 | I 0.90 | J 1.25 | H 1.62 | K 2.2 | L 3.4 |
|---|---|---|---|---|---|---|---|---|---|
| J I (Io) | 8.19 | 6.38 | 5.33 | 4.61 | 4.13 | 3.75 | 3.44 | 3.44 | 3.42 |
| J II (Europa) | 6.60 | 6.18 | 5.32 | 4.72 | 4.37 | 4.26 | 4.68 | 5.26 | 7.30 |
| J III (Ganymede) | 6.11 | 5.60 | 4.78 | 4.16 | 3.79 | 3.65 | 3.77 | 3.85 | 5.67 |
| J IV (Callisto) | 7.27 | 6.71 | 5.86 | 5.24 | 4.86 | 4.54 | 4.26 | 4.24 | 5.16 |

The *albedos* followed from: (a) the observed fluxes derived from the measured magnitudes; (b) the incident solar fluxes for each satellite; and (c) the assumption that the reflected radiation is spread uniformly over a hemisphere. The satellite radii adopted are taken from Kaula (1968); the mean heliocentric and geocentric distances of Jupiter were 5.365 and 4.372 A.U., respectively; the magnitude and colors of the sun were taken from Johnson (1964); and the photometric calibrations from Johnson (1966). The albedo thus obtained is a simplified Lambert-type, not equal either to the Bond or the geometrical albedo commonly used (Kaula 1968). The wavelength dependence shown in Figure 1 is not affected, of course. The visual albedos ($\lambda = 0.55\mu$) relative to Io are:

$$J\,II/\,J\,I = 1.32$$
$$J\,III/J\,I = 0.71$$
$$J\,IV/J\,I = 0.31$$

These ratios should also apply to the Bond and geometric albedos.

The curves of Figure 1 show a variety of features. For Io the albedo falls off rapidly to the ultraviolet, but remains high and nearly constant from the visual to $\lambda = 3.4\ \mu$; the high value at 3.4 $\mu$ does not favor a surface composition of $NH_4Cl$, but is compatible with a sulfur compound. The drop in the curves for Europa and Ganymede confirms earlier conclusions that $H_2O$ ice is present on these satellites (Kuiper 1957), while the decrease seen at 3.4 $\mu$ for Callisto could be due to $NH_4 \cdot Cl$.
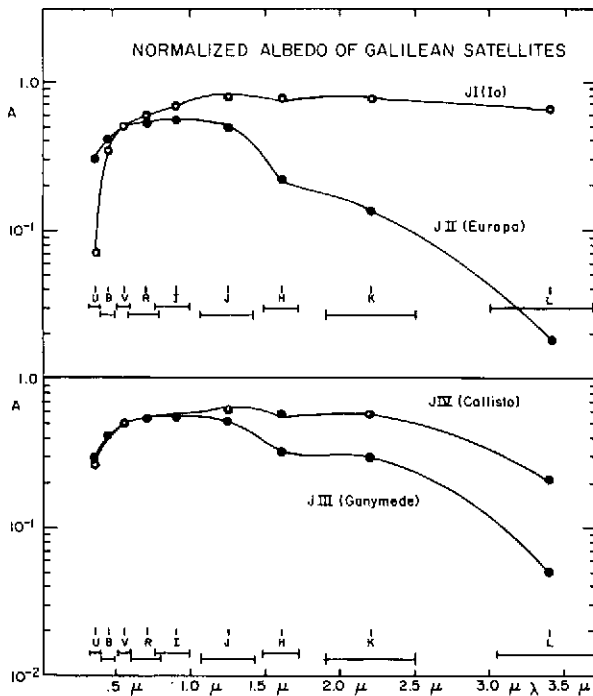
*Fig. 1. Normalized Albedos of Galilean Satellites.* The curves show the wavelength dependence of the albedo from $\lambda = 0.36\mu$ to $3.4\mu$. The various photometric band positions and their half widths are shown. The curves are normalized to A = 0.50 at $0.55\mu$.

## REFERENCES

Harris, D. L. 1961, "Photometry and Colorimetry of Planets and Satellites," in *Planets and Satellites*, eds. G. P. Kuiper and B. M. Middlehurst, (Chicago: University of Chicago Press), ch. 8, p. 272.

Johnson, H. L. 1964, "The Colors, Bolometric Corrections and Effective Temperatures of the Bright Stars," *Bol. Obs. Tonantzintla y Tacubaya*, 3, 305.

Johnson, H. L. 1966, "Astronomical Measurements in the Infrared," *Ann. Rev. Astr. Ap.*, 4, 193.

Kaula, W. M. 1968, *An Introduction to Planetary Physics: The Terrestrial Planets*, (New York: Wiley and Sons), p. 220.

Kuiper, G. P. 1957, "Infrared Observations of Planets and Satellites," *A.J.*, 62, 245.

# No. 169  MAP OF THE GALACTIC NUCLEUS AT 10μ

*by* G. H. Rieke and F. J. Low

September 2, 1971

## ABSTRACT

The galactic nucleus has been mapped at 10 microns with a resolution of a few arc seconds. Four discrete sources were resolved superimposed on an extended background.

We have scanned the center of our galaxy at a wavelength of 10 microns with a beam 5.5 arcsec in diameter. The scans have been combined to produce the map shown in Figure 1. At 10kpc, commonly assumed to be the distance to this region, 5.5 arcsec corresponds to 0.3 pc.

These observations were taken during the day on February 15, 1971, with the sixty-one-inch telescope at the Catalina Observatory. Because of the imprecision in the drive of the telescope, the scans could not be located accurately in declination; the telescope also drifted slowly in right ascension. These problems were overcome by comparing the scans with some made earlier by one of us (FJL) and D. E. Kleinmann with the Steward Observatory 90-inch telescope. Minor distortions may persist in the map. All of the features described below stand out clearly above the noise, which has a peak-to-peak value of about 6 x 10$^{-17}$ W/m$^2$ Hz ster.

Four sources can be distinguished and are numbered in Figure 1. An additional broad zone of emission can be seen extending to the north. Sources 2 and 4 are partially resolved and have diameters of about 0.5 pc. There are indications on the individual scans that Source 2 would break up into two or three sources at higher resolution. Source 1 is unresolved and must be less than 0.2 pc in diameter. Source 3 may also be unresolved with our beam, although the ratio of signal to noise is inadequate to permit a strong statement.
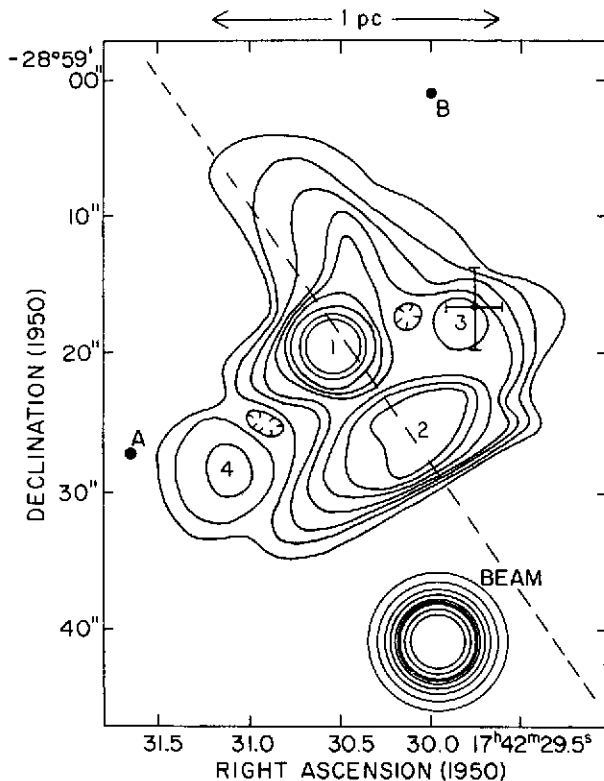
*Fig. 1*  Map of the galactic center at 10 microns. The peak-to-peak noise of the observations is 6 x $10^{-17}$ W/m² Hz ster. The contours are at levels of 1, 2, 4, 6, 8, 10, 12, 16 and 20 times this value. The brightest 10-micron sources are numbered in order of decreasing maximum flux. The beam used for these observations has a full width at half maximum of 5.5 arcsec. It is shown with the same contour levels as are used for the map. The location of the 2.2-micron "point-like" source is indicated by a set of error bars which correspond to the uncertainty in our measurement of its position. The two most prominent field stars have been plotted and labelled A and B. The direction of the galactic plane is indicated by the dashed line.

We have also made observations at 2.2, 5 and 22 microns. A detailed description of all this work will be published after we have analyzed it more completely. We have located the "point-like" source discovered at 2.2 microns by Becklin and Neugebauer (1968) relative to our map; to within the accuracy of the measurements, its position agrees with that of Source 3. At 5 microns, scans across the complex of sources have been made at five declinations. Although these scans have a relatively low ratio of signal to noise and are insufficient in number to construct a map, they do show the same general features found on the 10-micron map.

At 22 microns, we have constructed a map with the same resolution and nearly the same ratio of signal to noise as for the 10-micron map. The noise

for this map has a peak-to-peak value of about 1.8 x $10^{-18}$ W/m² Hz ster; at this level, Sources 2 and 3 were not detected. Source 1 stands out prominently. It lies near the center of an extended source that has a radius of about 20 arcsec.

Two field stars are plotted in Figure 1 and labeled A and B. Additional scans at 10 microns enabled us to locate our map relative to field star A. The coordinates of this star were measured from a Palomar Sky Atlas plate, allowing us to determine the absolute position of the 10-micron sources to within about 2 arcsec. (A finding chart for the galactic center has been published by Spinrad, *et al.*, (1971) (their Fig. 1). Star A is 2.5 mm south and 2.0 mm east of the indicated position of the galactic center on this chart and star B is 1.5 mm north and 1.0 mm west. It should be noted that the position of the 10-micron sources differs somewhat from the one indicated on the published finding chart.)

From our map, we estimate the total flux from the galactic center to be 480 ± 50 x $10^{-26}$ W/m² Hz at 10 microns. The 22-micron map indicates that the flux at this wavelength is 2300 ± 250 x $10^{-26}$ W/m² Hz, of which about 60% or 1400 ± 150 x $10^{-26}$ W/m² Hz would fall within a field of view 25 arcsec in diameter. These results are in reasonably good agreement with earlier measurements made with a 25 arcsec field of view of 550 ± 60 x $10^{-26}$ W/m² Hz at 10 microns, and 1700 ± 200 x $10^{-26}$ W/m² Hz at 22 microns (Low, Kleinmann, Forbes and Aumann, 1969).

Maps of the galactic center at 2.2 microns have already been published (Becklin and Neugebauer, 1968). At this wavelength the detected flux arises almost entirely from unresolved stars. Except for the "point-like" source, the brightest features at 2.2 microns would produce a flux of 0.2 x $10^{-26}$ W/m² Hz in a field of view the size of ours. At 10 microns, the flux from these stars should be an order of magnitude lower. Our peak-to-peak noise is about 3.5 x $10^{-26}$ W/m² Hz; thus, the general stellar background detected at 2.2 microns makes virtually no contribution to the 10-micron map. Becklin and Neugebauer (1969) have published the results of a scan across the galactic center at 10 microns. Their scan appears to have passed near the center of Source 2.

The 10-micron sources fall within the region of maximum intensity of the extended 2.2-micron source, which is centered (Becklin and Neugebauer, 1968) at $\alpha$ (1950) = $17^h$ $42^m$ $30^s$ ± $1^s$ and $\delta$ (1950) = $-28°$ 59.4 ± 0.1. Their position also agrees with that of the radio source Sgr A (Maxwell

and Taylor 1968), $\alpha$ (1950) $= 17^h\ 42^m\ 30\overset{s}{.}6 \pm 1^s$ and $\delta$ (1950) $= -28° 59' 14'' \pm 15''$.

Despite the consistency of these positions, significant ambiguities remain if one looks closely at the data. Our 22-micron map suggests that source 1 lies at the galactic center. On the other hand, a scan across the maximum of the 2.2-micron extended source, published by Becklin and Neugebauer (1969), places the greatest density of stars near Source 2. The 2.2-micron "point-like" object can be identified with Source 3; if it is, the 2.2-micron scan must be shifted in a direction which improves the correspondence with Source 2. The existence of Source 2 indicates that objects considerably cooler than normal stars lie very near the maximum 2.2-micron intensity. The contribution of these objects to the 2.2-micron flux is not known, leaving the position of the point of maximum stellar density uncertain.

Resolution of 6 arcsec at radio frequencies (Downes, private communication) reveals that Sgr A consists of two objects, one to the east and one to the west of our position for the infrared sources. The published position reflects the contribution of both sources.

*Acknowledgments.* The first measurements of the discrete sources in the galactic nucleus were made by

Low and D. E. Kleinmann (1970). These data were essential to our present efforts. We wish to thank A. A. Hoag for giving us a plate from the Palomar Atlas and E. Roemer for assistance in carrying out the measurements.

## REFERENCES

Becklin, E. E. and Neugebauer, G. 1968, "Infrared Observations of the Galactic Center," *Ap.J.*, 151, 145.

Becklin, E. E. and Neugebauer, G. 1969, "1.65 — 19.5-Micron Observations of the Galactic Center," *Ap.J.*, 157, L31.

Downes, D. 1971, private communication.

Low, F. J., Kleinmann, D. E., Forbes, F. F. and Aumann, H. H. 1969, "The Infrared Spectrum, Diameter, and Polarization of the Galactic Nucleus," *Ap.J.*, 157, L97.

Low, F. J. 1970, "Infrared Properties of Nuclei," *Semaine d'Etude sur les Noyaux des Galaxies,* Vatican City, April 13–19.

Maxwell, A. and Taylor, J. H. 1968, "Lunar Occultations of the Radio Source Sagittarius A," *Astrophys. Letters,* 2, 191.

Spinrad, H., Liebert, J., Smith, H. E., Schweizer, F. and Kuhi, L. V. 1971, *Ap.J.,* 165, 17.

No. 170  PRELIMINARY REPORT ON OPTICAL SEEING TESTS AT MT. LEMMON,
MARCH-JUNE 1971

*by* GEORGE V. COYNE, S.J.

August 1, 1971

ABSTRACT

One of the Lick Observatory Polaris telescopes was used to test seeing conditions at Mt. Lemmon. The preliminary results indicate that the seeing is not unlike that at Kitt Peak. Soundings of the air flow patterns across Mt. Lemmon under winter conditions were also made by flying smoke pots on tethered balloons to elevations of 500 feet. There does not appear to be any serious local turbulence.

As part of the preliminary development of the Mt. Lemmon Observatory, an optical seeing test program was begun with one of the six-inch Polaris telescopes used by Lick Observatory under the direction of Dr. Merle Walker for the testing of various prospective observing sites. The description of this instrument is given by Harlan and Walker (1965) and the results of tests made at various California sites (Walker, 1970) and at sites in Arizona, Baja California, Chile and Australia (Walker, 1971) have been published.

The test telescope, which had been most recently used at Kitt Peak, was obtained by us in January, 1971. It was mounted by Frecker and Arthur at Mt. Lemmon on the radar drum proposed as the site of the photopolarimetric 70-inch telescope (see Figure 22 of Kuiper, 1970). The telescope was first mounted on the catwalk at the west of the drum but vibrations were too severe there and it was moved to the north edge of the drum where it is mounted on a steel I-beam structure. The objective protrudes slightly over the north edge of the drum and is at an elevation of approximately 30 feet above the ground level. There are no wind breaks about the telescope or mounting.

During the period March 3 to March 16, six exposures of 15 minutes each were made per night, two each at $21^h$, $24^h$ and $3^h$ (MST); after March 16 three 15-minute exposures were made, one at each of the stated times.

TABLE I

Journal of Observations

| Date 1971 | Time (Start) MST | Film Roll | Exp. | Temp. °F | Rel. Hum. % | Wind Vel. | Dir. | Seeing (Sec. of Arc) | Obs. |
|---|---|---|---|---|---|---|---|---|---|
| March 3/4 | 21:05 | 1 | 1 | 34 | 40 | 0 | - | <0.7 | TK |
| | 21:20 | 1 | 2 | 34 | 40 | 0-5 | SSW | 0.7 | JG |
| | 00:20 | 1 | 3 | 33 | 45 | 5-7 | SSW | 0.8 | TK |
| | 00:35 | 1 | 4 | 22 | 45 | 5-7 | SSW | 1.2 | TK |
| | 03:05 | 1 | 5 | 32 | 45 | 5-7 | SW | 1.2 | TK |
| | 03:20 | 1 | 6 | 32 | 45 | 5-7 | SW | 1.8 | JG |
| 4/5 | 21:26 | 1 | 7 | 31 | 53 | 15 | SW | 2.0 | MH |
| | 21:43 | 1 | 8 | 31 | 53 | 15 | SW | 2.0 | MH |
| | 00:05 | 1 | 9 | 30 | 62 | 20 | SW | 2.5 | MH |
| | 00:20 | 1 | 10 | 30 | 62 | 20 | SW | 3.0 | MH |
| 5/6 | 21:00 | 1 | 11 | 20 | 55 | 5 | NW | 6.0 | JF |
| | 21:05 | 1 | 12 | 20 | 55 | 5 | NW | 6.0 | JF |
| | 21:15 | 1 | 13 | 20 | 55 | 5 | NW | 6.0 | JF |
| | 23:50 | 1 | 14 | 25 | 25 | 10-20 | NNW | 5.0 | JF |
| | 00:15 | 1 | 16 | 25 | 25 | 10-20 | NNW | 5.0 | JF |
| | 02:55 | 1 | 17 | 25 | 18 | 2-9 | NNW | 1.8 | JF |
| | 03:10 | 1 | 18 | 25 | 18 | 2-9 | NNW | 2.0 | JF |
| 9/10 | 21:28 | 2 | 2 | 29 | 41 | 0-5 | NW | 1.3 | JG |
| | 00:14 | 2 | 3 | 28 | 46 | 0-5 | NW | 1.5 | JG |
| | 00:30 | 2 | 4 | 28 | 46 | 0-5 | NW | 1.6 | JG |
| | 03:09 | 2 | 6 | 28 | 45 | 0-5 | NW | 2.0 | JG |
| | 03:21 | 2 | 7 | 28 | 45 | 0-5 | NW | 2.0 | JG |
| 11/12 | 21:08 | 2 | 8 | 32 | 44 | 0-5 | SSW | 1.5 | TK |
| 12/13 | 21:00 | 2 | 9 | 35 | 56 | 8-10 | S | 2.0 | MH |
| | 21:16 | 2 | 10 | 35 | 56 | 8-10 | S | 2.0 | MH |
| | 00:00 | 2 | 11 | 34 | 74 | 10-15 | S | 1.9 | MH |
| | 00:30 | 2 | 13 | 34 | 74 | 10-15 | S | 1.6 | MH |
| | 03:00 | 2 | 14 | 34 | 82 | 10-15 | S | 4.0 | MH |
| | 03:15 | 2 | 15 | 34 | 82 | 10-15 | S | 41.0-5.0 var | MH |
| 16/17 | 20:50 | 3 | 1 | 40 | 23 | 8 | S | 1.0 | JF |
| | 21:10 | 3 | 2 | 40 | 23 | 8 | S | 0.8 | JF |
| | 21:15 | 3 | 3 | 40 | 23 | 8 | S | 1.0 | JF |
| | 23:50 | 3 | 4 | 38 | 24 | 8 | S | 1.9 | JF |
| | 00:00 | 3 | 5 | 38 | 24 | 8 | S | 1.2 | JF |
| | 02:46 | 3 | 6 | 38 | 24 | 8 | S | 1.2 | JF |
| | 03:00 | 3 | 7 | 38 | 24 | 8 | S | 1.7 | JF |
| 17/18 | 21:04 | 3 | 8 | 34 | 29 | 15,gusts to 20 | SW | 5.0 | MH |
| | 00:00 | 3 | 9 | 32 | 34 | 20,gusts to 30 | W | 5.0 | MH |
| | 03:04 | 3 | 10 | 32 | 38 | 15,gusts to 20 | W | 5.0 | MH |

TABLE I

Continued

| Date 1971 | | Time (Start) MST | Film | | Temp. °F | Rel. Hum. % | Wind | | Seeing (Sec. of Arc) | Obs. |
|---|---|---|---|---|---|---|---|---|---|---|
| | | | Roll | Exp. | | | Vel. | Dir. | | |
| March | 20/21 | 21:35 | 3 | 111 | 32 | 25 | 0-5 | W | 1.5 | JF |
| | | 01:05 | 3 | 12 | 31 | 25 | 5 | SW | 1.3 | JF |
| | | 03:05 | 3 | 13 | 29 | 25 | 0-5 | SW | 1.6 | JF |
| | 27/28 | 20:50 | 3 | 14 | 42 | 56 | 8 | W | 1.3 | JF |
| | | 23:45 | 3 | 15 | 39 | 90 | 8 | W | 1.5 | JF |
| | | 02:50 | 3 | 16 | 36 | 72 | 6 | W | 1.5 | JF |
| April | 3/4 | 21:00 | 4 | 2 | 38 | 28 | 20 | N | 4.0 | JF |
| | | 00:00 | 4 | 3 | 37 | 27 | 5 | N | 4.0 | JF |
| | | 03:00 | 4 | 4 | 37 | 30 | 6 | N | 4.0 | JF |
| | 5/6 | 20:55 | 4 | 5 | 42 | 32 | 0 | - | 0.9 | TK |
| | | 23:56 | 4 | 6 | 36 | 30 | 0 | - | 0.8 | TK |
| | | 03:05 | 4 | 7 | 39 | 32 | 3 | W | 1.0 | TK |
| | | 03:20 | 4 | 8 | 39 | 32 | 3-6 | W | 1.0 | TK |
| | 6/7 | 21:10 | 4 | 9 | 43 | 38 | 7 | SE | 1.5 | JF |
| | | 23:45 | 4 | 10 | 42 | 43 | 10 | SE | 1.7 | JF |
| | | 02:45 | 4 | 11 | 39 | 38 | 4 | SSW | 1.2 | JF |
| | 7/8 | 23:50 | 4 | 13 | 37 | 27 | 5-25 | SW | 6.0 | JG |
| | | 02:55 | 4 | 14 | 36 | 38 | 10-30 | SW | 4.0 | JG |
| | 8/9 | 21:25 | 4 | 15 | 48 | 26 | 10-15 | SW | 1.5 | GC |
| | | 23:58 | 4 | 16 | 45 | 28 | 10-15 | S | 1.6 | GC |
| | | 02:45 | 4 | 16 | 42 | 34 | 10-15 | S | 1.5 | TK |
| May | 19/20 | 21:02 | 5 | 1 | 47 | 14 | 4 | S | 1.0 | MH |
| | | 00:00 | 5 | 2 | - | - | 5-10 | S | 1.0 | MH |
| | | 03:00 | 5 | 3 | - | - | 7-10 | S | 1.7 | MH |
| June | 3/4 | 21:00 | 5 | 5 | 36 | 58 | 8-10 | W | 5.0 | MH |
| | | 00:00 | 5 | 6 | 34 | 76 | 10-12 | S | 1.8 | MH |
| | | 03:00 | 5 | 7 | 36 | 58 | 10-12 | S | 1.5 | MH |
| | 9/10 | 21:00 | 5 | 8 | 46 | 52 | 8-10 | S | 2.5 | MH |
| | | 00:00 | 5 | 9 | 42 | 79 | 15-20 | SE | 1.7 | MH |
| | | 02:50 | 5 | 10 | 40 | 70 | 15-20 | SE | 3.0 | MH |
| | 29/30 | 21:06 | 5 | 11 | 55 | 30 | 0 | - | 1.5 | MH |
| | | 00:00 | 5 | 13 | 54 | 32 | 4-6 | S | 1.0 | MH |
| | | 03:00 | 5 | 14 | 54 | 30 | 7-10 | S | 1.0 | MH |

The following observers (identified by initials in Table 1) have participated in this program: George Coyne, Jack Frecker, John Gradie, Morris Howes and Thomas Kunkle. The exposed film rolls were sent to Dr. Walker who developed the film, compared the star trails to his standard calibrated trails, and sent to me the results listed in column 9 of Table I. Temperature and relative humidity were read by each observer from the hygrothermographs, which are monitored weekly by Ewen Whitaker. Wind velocity and direction were measured from a hand-held meter or read from a wind vane mounted at the west edge of the drum. The 25 percentile of the relative humidity by Table I is 27% (instrument reading); however, checks made with a psychrometer show that the instrument gave readings averaging about 4% too high.

Observations were made during a total of 19 nights during March-June, 1971. A journal of observations is given in Table I and the distribution of the average seeing for each night is given at the bottom of Figure 1. For each night the average seeing over all exposures was determined. However, for the nights of March 5/6, March 12/13 and June 3/4 the seeing changed by a large factor in the course of the night so that the last two exposures are treated as a separate night for each of these three nights. A total of 22 nights are, therefore, plotted in Figure 1. The average seeing over all nights is 2″1.

There are obviously too few observations from which to make any conclusive statements on the seeing at Mt. Lemmon. As a preliminary step, we make a comparison in Figure 1 between our Mt. Lemmon observations and those made at Kitt Peak with the same instrument for the same months, but for the two previous years. The information for Kitt Peak is from Walker (1971). At Kitt Peak the Polaris telescope was mounted on a concrete pier just west (up-wind) of the 36-inch No. 1 telescope, with its objective about 9 feet above ground level. The two years on Kitt Peak are sufficiently different to caution against general conclusions. All one can say is that the 1971 Mt. Lemmon run is not unlike the Kitt Peak runs made in 1969 and 1970.

It was feared that vibrations of the telescope by the wind might be introducing false seeing effects into the star trails, although there was no direct evidence for this, visually or photographically. In Figure 2 we have plotted the seeing for each individual exposure against the average wind at the time of that exposure. At wind velocities of 15 mph and less, a wind vibration effect cannot be very large, since both large and small seeing disks are observed. We cannot say what happens at higher velocities. In general, higher wind velocities are a sign of more turbulent conditions and poorer seeing. Therefore, we should expect some correlation between seeing and wind velocity even for a stationary telescope. For the present, the telescope appears to be adequately mounted for the average wind velocities encountered.

In addition to the seeing tests with the Polaris telescope, a sampling was made of air motion across the Mt. Lemmon summit. This was done by flying smoke pots on tethered balloons to elevations of 500 feet and observing the flow pattern of the smoke at various elevations. All flights were made from or near the same radar drum on which the Polaris telescope is mounted. The general results are:

(1) The flow from the eastern quadrants is laminar for wind velocities up to 30 mph.

(2) The air flowing up the steep western slope remains parallel to the ground and does not appear to be turbulent. It passes the drum on the summit, some 30 meters (70 ft.) from the west rim, at the same slope angle as the western slope itself, i.e. it does not curl over the drum.
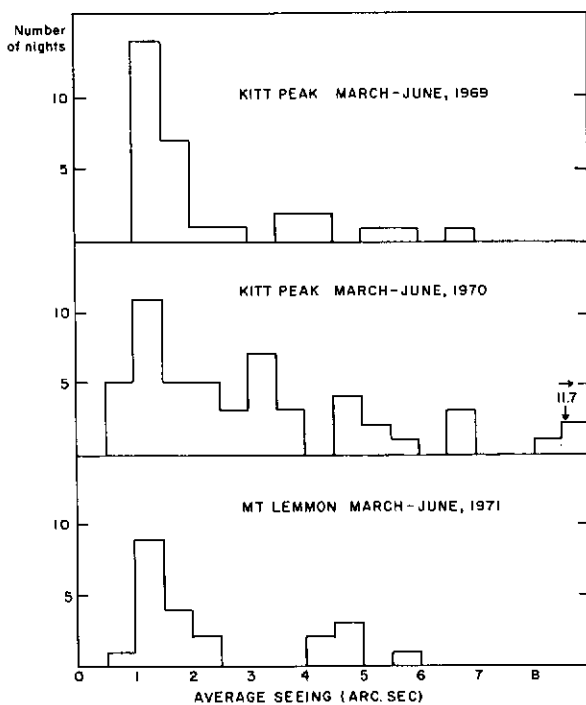


*Fig. 1* Distribution of the average seeing (in seconds of arc) per night at Mt. Lemmon and at Kitt Peak during the same season but for different years.
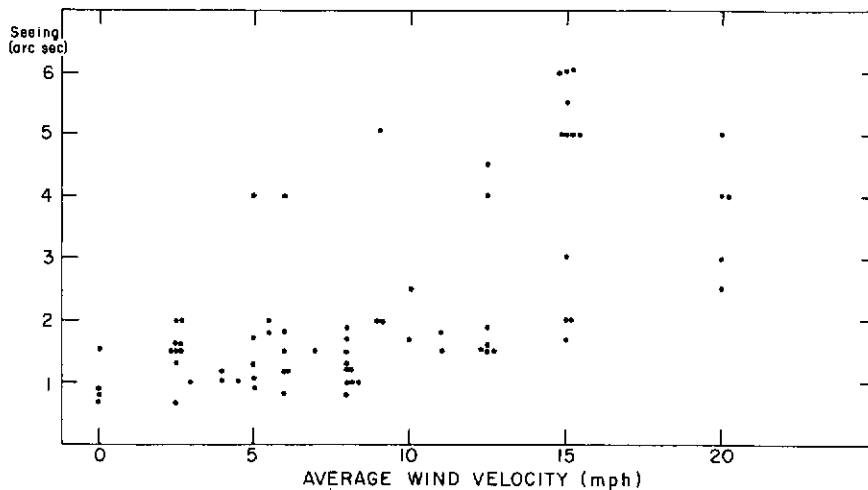
*Fig. 2*  Estimated seeing (in seconds of arc) plotted versus wind velocity for each individual observation.

(3) The air from the west above this boundary layer flows horizontally at elevations examined up to 500 feet above the drum.

(4) By observing yellow smoke moving upslope at ground level and black smoke moving in from the west horizontally at the level of the drum, we attempted to study what happened at the interface of these two currents. The results are not altogether conclusive but there does not appear to be any serious turbulence. There were certainly no observable eddies and curls where the two currents met at the drum.

(5) All of these tests were made under winter conditions (free air temperatures less than 60°F); warmer air may behave differently. There is no prominent local air turbulence at the location tested.

## REFERENCES

Harlan, E. A. and Walker, M. F. 1965, "A Star-trail Telescope for Astronomical Site-testing," *Pub. A. S. P.*, 77, 246.

Kuiper, G. P. 1970, "High Altitude Sites and IR Astronomy, II," *LPL Comm.* No. 156, 8, 337-383.

Walker, M. F. 1970, "The California Site Survey," *Pub. A. S. P.*, 82, 672.

Walker, M. F. 1971, "Polar Trail Observations of Astronomical Seeing in Arizona, Baja California, Chile and Australia," *Pub. A. S. P.*, 83, 401.

## No. 171  SULFURIC ACID IN THE VENUS CLOUDS

*by* GODFREY T. SILL, O. CARM.

December 15, 1972

### ABSTRACT

The extremely dry nature of the Venus upper atmosphere appears to demand the presence of an efficient desiccating agent as the chief constituent of the clouds of Venus. On the basis of polarization measures one would expect this substance to be present as spherical droplets, $1\text{-}2\mu$ in diameter, with a refractive index $n$ of $1.46 \pm 0.02$ at 3500Å in the observed region of the atmosphere, with $T \sim 235°K$. This substance must have ultraviolet, visible and infrared reflection properties not inconsistent with the observed spectrum of Venus. Sulfuric acid, of about 86% by weight composition, roughly fulfills the first of these properties. The visible and ultraviolet transmission features of a thin layer of elemental bromine and hydrobromic acid dissolved in sulfuric acid somewhat resemble the Venus spectrum, up to $14\mu$. The chemical process postulated for forming sulfuric acid involves the oxidation of sulfur and its compounds to sulfuric acid through the agency of elemental bromine, produced by the photolytic decomposition of hydrogen bromide.

### 1. Current data on the Venus Clouds

Substantial data exist on the spectroscopic and polarimetric properties of the Venus clouds. Yet the identity of the clouds is still uncertain. Venus shows high reflection of visible light, with an albedo approaching 100%. There are strong absorption features in the ultraviolet and infrared, independent of the atmospheric absorptions caused by $CO_2$. Ultraviolet photography of the planet shows regions of variable darkness, attributed to different cloud layers on the planet, revealing a dynamic system of production and destruction of a strong ultraviolet absorber, produced photolytically in the upper atmosphere. It is important to remember that the high resolution UV spectroscopy of the planet utilizes the average reflection of the whole planet in the ultraviolet. Figure 1 shows the albedo of Venus from 0.2 to $4.0\mu$, as taken from Kuiper's 1969 article on the clouds of Venus, with the UV region modified by Wallace *et al.* (1972), and the $3\text{-}4\mu$ region to allow for the $CO_2$ absorption $3.7\text{-}4.0\mu$ observed by Beer *et al.* (1972). A double absorption near $3.8\mu$,
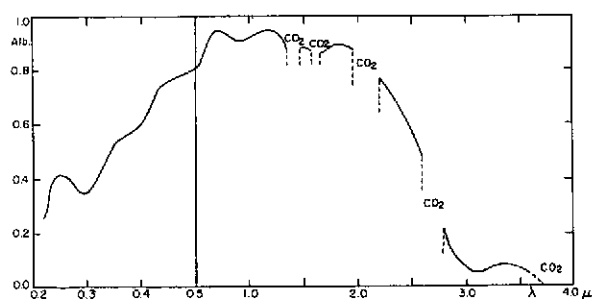
*Fig. 1*   Venus Bond albedos vs. wavelength, 0.2-4 $\mu$.

assumed by these authors to be due to solid particles, is actually due to $CO_2$ gas (Kuiper 1972).

Polarization studies by Coffeen (1968) led him to conclude that the particles in the clouds were probably spherical, with a refractive index $n$ of 1.43-1.60 and a mean particle size of 2.5$\mu$. Further work by Hansen and Arking (1971) and Coffeen and Hansen (1972) give a mean particle size of 1.1$\mu$ and $n$ of 1.46 $\pm$ 0.02 at 0.35$\mu$ decreasing to 1.43 at 1.0$\mu$. The particles are spherical, and show other properties of spheres, the rainbow and possibly the glory.

Another important property of the Venus atmosphere at the level of the clouds, namely at 50 mb pressure ($10^{-1.30}$atm) and 235°K, is the extremely low water vapor mixing ratio of $10^{-6.0}$($P_{H_2O} = 10^{-4.30}$mb). The vapor pressure of ice is higher than this value by orders of magnitude. If $H_2O$ is a constituent of the clouds, it must be present with a strong desiccating agent. Kuiper (1969) in suggesting $FeCl_2 \cdot 2H_2O$ as a constituent of the Venus clouds made the cogent observation that the vapor pressure of water in $FeCl_2 \cdot 2H_2O$ at 250°K was compatible with the observed vapor pressure of water. This property is not unique to $FeCl_2$, however. Other possible desiccating agents can fulfill this function.

Is there any one substance that can account for all the above properties of the clouds as well as being compatible with the albedo of Venus over the spectrum? $FeCl_2$ does a creditable job for some parts of the spectrum, but not all. $FeCl_2$ does not satisfy the polarimetric properties because it tends to form hexagonal platy crystals, not spheres.

The author was intrigued by the fact that Fe $SO_4$ hydrate, as well as other hydrated sulfates, showed low reflectivity between 3.0 to 4.0$\mu$ in the infrared. No other hydrates did as well in satisfying the low reflectivity of Venus in this region. An obvious candidate for consideration as a cloud constituent was

$H_2SO_4$, which also showed strong absorption in the 3 to 4$\mu$ region.

The above considerations led to an interim report dated 24 March 1972, sent to NASA and scientific colleagues, prepared by Dr. Kuiper, from which we quote:

> "Mr. Sill found that elemental sulfur may form a cloud layer in the deeper atmosphere. In any case, sulfur-dioxide will penetrate into the upper atmosphere, where it could be oxidized to sulfuric acid by free halogens, particularly iodine; and there possibly form small cloud particles in the upper Venus atmosphere composed of sulfuric acid, of 88% concentration. This concentration would be consistent with the observed $H_2O$ mixing ratio. The refractive index of this sulfuric acid solution would be about 1.45 at 240°K, in agreement with the polarization data. This material would supercool into spheres, as also indicated by the observed polarization properties of the planet. This explanation for the Venus clouds could be either an alternative to the $FeCl_2 \cdot 2H_2O$ explanation advanced in *LPL Comm. No. 101* or possibly apply to the UV cloud layer only and thus be in addition to the ferrous-chloride explanation for the yellow lower clouds. In either case, the reflection spectra should be obtained next year of sulfuric acid fogs produced in the laboratory, both with and without dissolved halogens."

Another section of this report is also quoted:

> "Mr. Sill found that the observed $CO/CO_2$ ratio of about $10^{-4.3}$ may be explained as due to an equilibrium reaction involving the weathering of iron-bearing olivines and pyroxenes by carbon dioxide:

$$CO_2 + Fe_2SiO_4 = Fe_2O_3 + SiO_2 + CO. \qquad (1)$$
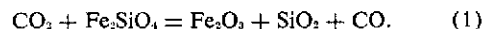
> At $T_s = 750$°K and $P_s = 100$ atm. the $CO/CO_2$ ratio according to thermodynamics should indeed be about $10^{-4.3}$.
>
> "Mr Sill found that the abundances of the acid halides (HF and HCl) may be explicable if one considers an equilibrium with a surface deposit of calcite, the latter being called upon to explain the abundance of $CO_2$. Carbonates are attacked by acid halides,

$$CaCO_3 + 2HX = CaX_2 + H_2O + CO_2, \qquad (2)$$
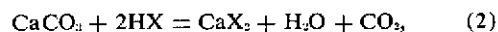
> where $X = F$, Cl, Br, or I. With the ratio $H_2O/CO_2 = 10^{-6}$ found in the upper atmosphere, HCl and HF would indeed have the mixing ratios of $10^{-6}$ and $10^{-8}$, as observed. If on the other hand, elemental abundances were solely responsible one would expect HCl to be only 5 times more abundant than HF. Therefore, it would follow that the process of eq. (2), rather than the abundance ratios, determines the relative amounts of HCl and HF. If the $H_2O/CO_2$ ratio in the lower atmosphere is well in excess of $10^{-6}$, this could imply that the acid halides also would be more abundant there.
>
> "If HBr and HI are used in eq. (2), then the equilibrium amounts of HBr and HI are found to be an order of magnitude more than HCl; though here elemental abundances may affect the total bromine and iodine availability. Furthermore, HBr and HI are less stable than HCl, and tend to break down upon exposure to UV (sun) light around 2500Å.
>
> "An observational program was therefore initiated for the detection of $Br_2$ or HBr on Venus. The strong HBr absorption at 2.0 lies in the middle of very intense Venus $CO_2$ absorptions. However, $Br_2$ has a strong electronic band in the accessible region, 3600-5500Å, with a maximum absorption at 4100Å. This absorption causes the gas to be strongly colored visually. The band structure of $Br_2$ is most readily seen between 5300-

5400Å, since the absorption is nearly continuous near its maximum. If the yellow tint of Venus were due to gaseous $Br_2$, only ½ mm atm. would be required. This amount would just be detectable on Venus with an existing LPL spectrograph having 4A/mm dispersion, as observed between the sun's Fraunhofer lines. Spectra of Venus were obtained with this instrument on the 61-inch telescope, Catalina Observatory. No detectable $Br_2$ absorptions were found between 5100-5400Å. However, the $Br_2$ absorptions are so numerous and sharp that high resolution on Venus is called for. This problem is being pursued."

The present publication updates these preliminary results.

The first property to verify was the vapor pressure of water in equilibrium with various $H_2SO_4$ solutions at 235°K. The INTERNATIONAL CRITICAL TABLES give values of $P_{H_2O}$ over $H_2SO_4$ solutions from 10 to 95% $H_2SO_4$. The appropriate values seemed to be in the high $H_2SO_4$ concentrations. At 235°K the following were calculated:

| % (wt) $H_2SO_4$ | Log $P_{H_2O}$ of soln. (mb) |
|---|---|
| 90 | −5.03 |
| 85 | −4.14 |
| 80 | −3.56 |

Since log $P_{H_2O}$ (mb) at the cloud level is −4.3, the 85% $H_2SO_4$ solution is close to the observed value, with 86% solution a good fit. More exhaustive analysis of water vapor regulated by $H_2SO_4$ was performed by Fink, Larson, et al. (1972). They found $H_2SO_4$ of about 80% composition can dry the upper atmosphere to give good agreement with the measured abundance of $H_2O$.

The second property to consider is refractive index $n$. The INTERNATIONAL CRITICAL TABLES list refractive index for $H_2SO_4$ solutions (particularly 95-96% solutions) at various temperatures and wavelengths. From 301 to 387°K the refractive index decreases linearly with temperature increase. Extrapolating back to 235°K, and correcting for wavelength, $n$ for 95-96% $H_2SO_4$ at 3500Å is 1.440. With the $n$ value of 1.405 for $H_2SO_4 \cdot 2H_2O$ (73%) at 20°C (HANDBOOK OF CHEMISTRY AND PHYSICS), the 235°K $n$ value should be 1.419. The 86% $H_2SO_4$ solution would therefore be calculated as $n = 1.431$ at 235°K. This value is close to the 1.46 ± 0.02 of Coffeen and Hansen, but somewhat outside the limit. Solutions of $H_2SO_4$ > 95% are compatible with the polarization measurements. It well might be that the spherical droplets are actually frozen. This would raise the refractive index of 86% $H_2SO_4$ to about 1.453, well within the acceptable limits. $H_2SO_4$ freezes in a com-

plex manner, with various eutectics ($H_2SO_4 \cdot H_2O$, $H_2SO_4 \cdot 2H_2O$, $H_2SO_4 \cdot 4H_2O$) freezing at various temperatures, and mixtures of them freezing at lower temperatures. Pure $H_2SO_4$ freezes at 10.5°C, the monohydrate at 8.6, the dihydrate at −38.9°, the tetrahydrate at −24.5°.

The author has observed in the laboratory the freezing and melting properties of an 88% $H_2SO_4$ solution. The frozen $H_2SO_4$ seemed to have an ill-defined melting point, it appeared to just become less viscous as it melted, behaving almost like a glass. A thin layer of the acid was frozen in dry ice and was perfectly transparent. The surface looked glassy. A cold metal spatula seemed to dent the surface; no fractures were observed as is common with water ice. The cloud particles of Venus could therefore be of this "glassy" type $H_2SO_4$, the droplets frozen into spheres, with a refractive index indicative of this denser state, namely about 1.45.

The third property of $H_2SO_4$ to compare with the clouds of Venus is spectral reflectivity. As of this time it has not been possible to obtain reflection spectra from fogs of $H_2SO_4$. As a second best choice, transmission spectra of thin layers of $H_2SO_4$ might simulate to a degree the complex absorption and scattering occurring in a fog of droplets. The thin layer of $H_2SO_4$ was obtained by putting a drop of the acid between two plates and letting them seal together. Excess acid was usually squeezed out around the edges of the plates. It is estimated that the layer of acid is approximately 0.05 mm thick. Two plates of optical quartz, each 2 mm thick were used in the transmission spectra from 0.2 to 3.5μ. AgCl plates, ground and polished, were utilized in the spectral region 2.5 to 15.0μ. Also used in this region, with less success, were drops of $H_2SO_4$ sandwiched between layers of polyethylene and Saran. The absorptions of the plastics were added to $H_2SO_4$, of course. This was partially cancelled in the dual beam spectrophotometer by placing two layers of plastic in the reference beam, but complete cancellation of the plastic film does not appear to be possible. Instrumental effects near the strong and sharp absorption features of the plastic film produce spurious features in the $H_2SO_4$ spectrum. The 0.2 to 3.5μ spectra were obtained from a Beckman DK-2A dual-beam quartz spectrophotometer, and the 2.5 to 15.0μ spectra from a Perkin-Elmer 137 NaCl spectrophotometer, both used by courtesy of Dr. B. Nagy of the University of Arizona's Department of Organic Geochemistry.
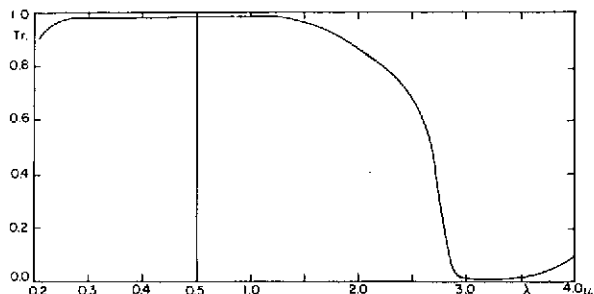
*Fig. 2* Transmission spectrum of 88% H₂SO₄, 0.05 mm thick.

Figure 2 shows the spectral transmittance of a thin layer of 88% H₂SO₄. The two quartz plates were used with an acid layer about 0.05 mm thickness between the two plates. The reference beam was the air path. The spectrum needed only very small correction for the absorption of the two quartz plates. By comparison with the Venus spectrum, Figure 1, it can be seen that there is a good match from about 1-3μ. Obviously the ultraviolet and visible spectral region must be explained by some other substance(s). Among possible candidates for ultraviolet absorptivity is $SO_2$ dissolved in cold $H_2SO_4$. Since S is oxidized to the 6+ oxidation state in $H_2SO_4$, the intermediate oxidation state of 4+ in $SO_2$ should be expected. The visible yellow color of the Venus clouds presents a problem as well. There are not too many gaseous substances which have a yellow tint. One is brown-yellow $NO_2$. But at the temperature of the Venus clouds the dimmer $N_2O_4$ is highly favored, with a consequent drastic lessening of color intensity. Furthermore, it may be extremely difficult to oxidize N in the atmosphere of Venus. A better candidate is $Br_2$; a red-brown liquid or gas, which if diluted and dissolved in $H_2SO_4$ to a moderate degree produces a yellow solution; higher concentrations give a red-brown solution. The intensity of the color of $Br_2$ varies with temperature. $Br_2$ saturated in 88%

$H_2SO_4$ solution at room temperature produces a red-brown solution; when cooled to dry ice temperatures, the frozen solid is yellow. The chemical aspects of $Br_2$ and $H_2SO_4$ will be discussed below.

Figure 3 shows the inferred Bond albedo of Venus in expanded scale from 0.2 to 0.6μ. Wallace (personal communication), from his geometric albedo in the rocket UV, estimates that the Bond albedo of Venus is about 0.4 at 2500Å. Figure 4 shows the transmittance of $Br_2$ and HBr dissolved in $H_2SO_4$; HBr was added to the $Br_2$ to dissolve more $Br_2$ than water alone would dissolve. The HBr + $Br_2$ solution was added to cold concentrated $H_2SO_4$ to obtain a solution of 88% $H_2SO_4$. Outgassing of HBr from the solution was rather vigorous. Solution B was more concentrated than A in $Br_2$ and showed more yellow color. Evidently even more coloring agent ($Br_2$) could be present than in solution B to match Venus 0.3-0.5μ; while the higher UV reflectance of Venus could be due to scattering. However, Venus has a UV peak near 2500Å, whereas the $Br_2$ solution peaks at 2200Å and the UV scattering would tend to displace it shortward. The Venus spectrum shows a dip at about 2900Å, whereas $Br_2$ solution dips at 2700Å, which would also be slightly displaced shortward by UV scattering.

The $SO_2$ spectrum is shown in Figure 5. In curve A, $SO_2$ gas was bubbled into cold 88% $H_2SO_4$ and a layer about 0.1 mm thick was observed through the quartz plates. The $SO_2$ does show a peak at 2400Å and a dip centered at 2800Å, somewhat closer to the Venus absorption and reflection. To observe the effect of a greater amount of dissolved $SO_2$ than could be held by the $H_2SO_4$ at room temperature, a cell of 88% $H_2SO_4$, 1 cm thick, was utilized with the $SO_2$ at about 1/200 of saturation. A similar cell with pure 88% $H_2SO_4$ was used in the reference beam of the Beckman DK-2A.
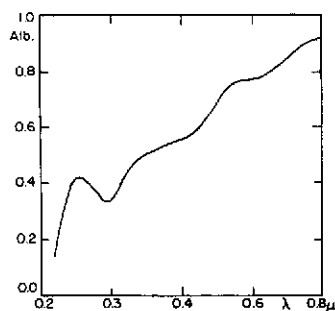


*Fig. 3* Venus Bond albedo vs. wavelength, 0.2-0.6 μ.
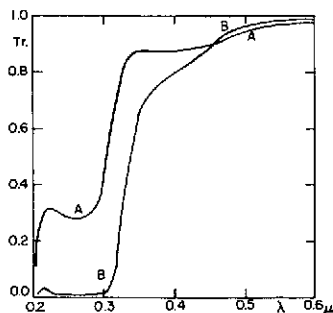


*Fig. 4* HBr + Br₂ dissolved in 88% H₂SO₄ (two concentrations).
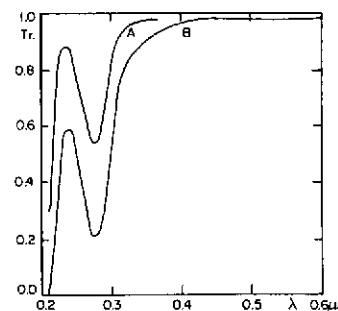


*Fig. 5* SO₂ dissolved in 88% H₂SO₄ (two concentrations).

When $Br_2$ vapor is poured onto a $SO_2$-$H_2SO_4$ solution, immediate bleaching of the $Br_2$ is observed, as well as a diminution of the absorption features of $SO_2$. Depending on which constituent survives, the spectrum either resembles the $SO_2$ or the $Br_2$ spectrum more closely. Evidently the $Br_2$ oxidizes the $SO_2$ to $H_2SO_4$ and the $Br_2$ is reduced to HBr.

Figure 6 shows the infrared spectrum from 4.0 to $15.0\mu$ of 88% $H_2SO_4$ (solid line) with the left hand ordinate of transmittance. The sample was one drop of acid squeezed between AgCl plates, with similar plates in the reference beam. The dashed spectrum of Venus is that of Gillett, Low, and Stein (1968) with the right-hand ordinate of log power at the detector. The dotted lines are, first, the reflection of sunlight from a body of unit albedo, and second, the black-body radiation curve at 225°K. If there is $H_2SO_4$ in the clouds cooler than the emitting surface, then indeed $H_2SO_4$ should show in absorption. There are some similarities between the absorptions of the Venus spectrum 7-12$\mu$ and the absorptions of 88% $H_2SO_4$, especially in the absorption feature centered at 11.2$\mu$, prominent in Hanel's Venus spectrum (1968).

## 2. Chemical Production of the $H_2SO_4$ Clouds

The mode of production of $H_2SO_4$ in the Venus atmosphere poses a complex problem. First of all no S compounds have been detected on Venus as gases. Upper limits to the mixing ratio of S compounds are available, and the values are (Kuiper 1969): $SO_2 < 10^{-7.5}$, $COS < 10^{-8}$, $H_2S < 10^{-3.7}$. Two of these compounds can probably be ruled out because of their instability to ultraviolet radiation in the upper atmosphere of Venus. $H_2S$ was exposed to the UV radiation of a quartz mercury penlight (most effective radiation at the Hg 2536.5Å). Within minutes, noticeable deposition of S particles on the walls of the flask was observed as well as a fine smoke of S in the gas. Within an hour decomposition was virtually complete. COS is almost as unstable to UV as $H_2S$, decomposing into CO and S. This decomposition also approaches 100% in hours. Since the upper Venus atmosphere appears transparent to $\lambda > 2000$Å, $H_2S$ and COS can be ruled out. This leaves one with $SO_2$ and S as the most likely carriers of S to the upper atmosphere.

$SO_2$ has S in the 4+ oxidation state; in order to produce $H_2SO_4$ it is necessary to oxidize S to the 6+ state, as found in $H_2SO_4$, or in the anhydride of $H_2SO_4$, $SO_3$. (The $SO_3$ would quickly absorb water
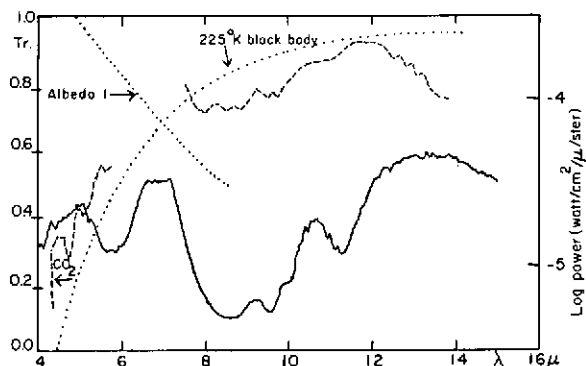


*Fig. 6* Solid line: Transmission spectrum with 88% $H_2SO_4$ solution (left ordinates). Dashed line: Infrared spectrum of Venus with black body and unit albedo references (right ordinates).

and form $H_2SO_4$). Is it possible to produce $SO_3$ in the Venus atmosphere? The process would be:

$$SO_2 + CO_2 = CO + SO_3. \qquad (1)$$

The resulting log $K$ values are $-32.64$, $-24.43$, $-16.40$, and $-13.14$ for the temperatures of 298°, 400°, 600°, 750° K, respectively. The thermodynamic data for calculating the equilibrium constant, $K$, are from Robie and Waldbaum (1968). With the $CO_2$/CO ratio of $10^{4.34}$ of Venus, presumed to be constant throughout the atmosphere, it is possible to calculate the $SO_2$/$SO_3$ ratio for the lower atmosphere (T > 400°K) where thermodynamics can furnish valid information The ratios for 298°K are included simply to show the trend:

| Temp. °K | 298 | 400 | 600 | 750 |
|---|---|---|---|---|
| $SO_2$/$SO_3$ ratio | $10^{28.32}$ | $10^{25.09}$ | $10^{12.06}$ | $10^{8.80}$ |

The ratio is *unfavorable* for $SO_3$ production *at any level*, let alone the upper atmosphere. In the lower hotter atmosphere it appears that the most abundant S species would be COS, $SO_2$, and $S_2$, in that order. It is impossible to give accurate ratios of the S compounds without knowing what the total S abundance is, and whether or not the $CO_2$/CO ratio remains constant. One possible surface reaction which might determine the abundance of atmospheric $SO_2$ involves the equilibrium decomposition of anhydrite, $CaSO_4$, in a $CO_2$-CO atmosphere:

$$CaSO_4 + CO = CaCO_3 + SO_2. \qquad (2)$$

At a surface temperature of 750°K, thermodynamics predicts a CO/$SO_2$ ratio of 10. The $CaSO_4$-$CaCO_3$ equilibrium was chosen because $CaCO_3$ is often considered as the major weathered mineral in a $CO_2$

atmosphere. Furthermore $CaSO_4$ is often found as a principal S compound in geothermal regions, indicating its ability to survive under moderately high temperature conditions. If the $CO/SO_2$ ratio of 10 should survive to the upper atmosphere there would be an abundant supply of $SO_2$ for forming $H_2SO_4$, provided there is a mechanism for further oxidizing the S to $SO_3$-$H_2SO_4$.

The oxidizing agent in the earth's atmosphere for converting $SO_2$ to $SO_3$ is $O_2$. On Venus this is ruled out, and the most likely agents are molecular halogens, namely $F_2$, $Cl_2$, $Br_2$ and $I_2$. $F_2$ can be rejected because of the extreme chemical stability of HF. Likewise $Cl_2$ gas must be rejected because HCl does not photolytically dissociate for $\lambda > 2000$Å. The spectra of HCl solutions show no notable absorptions in the ultraviolet between 2000-4000Å. HBr and HI are strong absorbers. Both gases are readily dissociated into hydrogen gas and the molecular halogen under Hg vapor irradiation, and a few hour's radiation brings about equilibrium. In the case of HBr:

$$2HBr \overset{h\nu}{=} H_2 + Br_2, \qquad (3)$$

equilibrium quantities of the gases indicate that 7% of HBr is decomposed in the gas-gas equilibrium. The aqueous solution of HBr also shows a noticeable darkening due to formation of $Br_2$ under UV exposure.

Mention was made of the bleaching effect of $SO_2$ gas dissolved in $H_2SO_4$ when $Br_2$ fumes were poured onto the surface of the acid-$SO_2$ solution. This apparently shows the ease at which $Br_2$ will oxidize $SO_2$ to $H_2SO_4$ in an acid medium. The thermodynamics also indicate a favorable reaction (Latimer 1952):

$$Br_2(liq) + H_2SO_3(aq) + H_2O =$$
$$2Br^-(aq) + 4H^+(aq) + SO_4^{2-}(aq) \; E_0 =$$
$$+0.89 \; volts. \qquad (4)$$
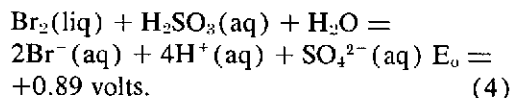
With a positive potential of 0.89 v, the reaction should and does proceed rapidly at room temperature. The two reactions can be summarized as:

$$2HBr = H_2 + Br_2 \qquad (5)$$
$$Br_2 + SO_2 + 2H_2O = H_2SO_4 + 2HBr.$$
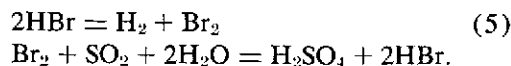
The HBr is reconstituted in the process, and in effect serves as a carrier catalyst for the reaction. The overall reaction therefore involves destruction of $H_2O$ into $H_2(g)$, which presumably escapes from Venus, and oxygen incorporated into $H_2SO_4$:

$$SO_2 + 2H_2O = H_2SO_4 + H_2. \qquad (6)$$

Reaction (6) is not favored thermodynamically and could never occur at the low temperature of the Venus clouds, but the intermediate reaction with $Br_2$ (and presumably the other halogen, $I_2$) make the process possible. None of the intermediate substances has been identified in the atmosphere of Venus, namely $SO_2$, HBr and $Br_2$. HBr is a difficult problem spectroscopically because its absorption bands at 2 and 4 microns fall into the heavy $CO_2$ bands. $Br_2$ (gas) was examined at our laboratory with the helpful assistance of Allen Thomson and Thomas N. Gautier. Moderately strong absorption bands were found in the region of 5364Å. Sill, Gautier, and Kuiper attempted to detect gaseous $Br_2$ in the atmosphere of Venus first with the 61-inch telescope of the Catalina Observatory, then with the 107-inch telescope of the McDonald Observatory. Edwin S. Barker of the University of Texas graciously aided us in obtaining high resolution spectra at the Coudé focus of the 107-inch telescope with its attendant echelle grating spectrograph. Spectra of Venus, the sun, and the sun + $Br_2$ (gas) were obtained in the region of 5364Å. The results were negative. From the spectra it is estimated that the smallest quantity of $Br_2$ that could be seen in Venus is about 0.13 mm-atm. *An upper limit to the Venus mixing ratio* $Br_2/CO_2$ can be set at $< 10^{-7.3}$. This implies a very small quantity of $Br_2$ vapor, much less than the 4 mb vapor pressure of elemental $Br_2$ at 235°K. On the other hand $Br_2$ is very soluble in cold $H_2SO_4$, especially in the presence of HBr.

Both $Br_2$ and $SO_2$ have mixing ratios with upper limits $< 10^{-7}$. This may simply be a sign of their high reactivity with each other. The reaction is fast and involves reconstituting HBr. Since no upper limit on HBr has been established, the whole postulated mechanism cannot be proven at this time. The empirical data discussed above indicate that the visible and UV albedos of Venus may be consistent with $Br_2$ dissolved in $H_2SO_4$. The highly sensitive test for gaseous $Br_2$ is not applicable to dissolved $Br_2$ as the sharp lines of the gas are smeared into the broad band of a liquid.

Chemical considerations would lead one to suspect that HBr is a gaseous constituent of the atmosphere of Venus, chiefly because HF and HCl are present. In general one halogen implies the presence of the others, taking due account of their chemical activity. A perfect case in point is the relative abun-

dance of HCl and HF in the Venus atmosphere, with mixing ratios of $10^{-6.0}$ and $10^{-8.0}$ respectively. The Cl/F ratio in the atmosphere is 100, whereas the cosmic elemental abundance ratio of Cl/F is 5.5 (Suess-Urey) or 1.8 (Cameron) according to the HANDBOOK OF PHYSICAL CONSTANTS. Something is making F less abundant in the atmosphere. Sea water on earth shows a similar disparity with a Cl/F ratio of 7000. In this latter case the explanation is due to the higher solubility of chlorides vs fluorides, plus the relative stability of fluoride micaceous minerals versus the chloride. As far as Venus is concerned, the relative solubilities of chlorides and fluorides in water have no bearing on the case, but rather the chemical stability of chloride and fluoride minerals in the presence of a hot $CO_2$ atmosphere. Pertinent reactions might be:

$$CaCl_2 + CO_2 + H_2O = CaCO_3 + 2HCl \atop CaF_2 + CO_2 + H_2O = CaCO_3 + 2HF. \quad (7)$$
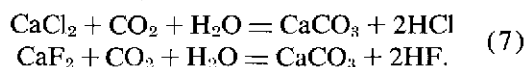
At 750°K, with $P_{CO_2}$ at 100 atm, the relative amounts of gaseous hydrogen halides, HCl/HF, is about 100, which is the observed ratio in the upper atmosphere. The simple cosmic abundance ratio is not valid. The same argument can be applied to the equivalent bromide:

$$CaBr_2 + CO_2 + H_2O = CaCO_3 + 2HBr. \quad (8)$$
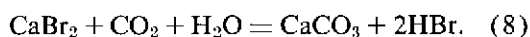
The ratio HCl/HBr is less than 1. It is possible that HBr might be more abundant than HCl in the Venus atmosphere if the surface reactions are the dominant influence in atmospheric abundance. This may be the case, otherwise HCl should be more abundant than the observed mixing ratio of $10^{-6.0}$. Cl in the earth's oceans amounts to $8.6 \times 10^{22}$ moles, whereas in Venus' atmosphere there is about $1.3 \times 10^{16}$ moles. Unless severe depletion of Cl occurred on Venus vs earth, the excess Cl on Venus should be locked in the surface rocks in a way similar to equation (7). When one considers Br on Venus, there might appear to be a problem of the absolute abundance of Br. The Cl/Br ratio in the earth's oceans is 660, which ratio is the one assumed by Suess-Urey as the relative cosmic abundance. If the absolute abundance of Br on Venus matches that in the earth, there is more than enough Br to make the equilibrium of equation (8) applicable, namely HBr would be more abundant in the atmosphere than HCl. Similar arguments can be applied to I, and HI would be thermally unstable and decompose.

### 3. Forming $H_2SO_4$ Synthetically in the Laboratory

Tests were conducted in the laboratory to see if $H_2SO_4$ could be formed by the irradition of HBr and S compounds. Acid solutions of HBr and various S gases, particularly $SO_2$ and COS were irradiated with the quartz Hg lamp. COS vigorously decomposed, producing large quantities of S. Some $H_2SO_4$ was produced, which was analyzed by precipitating $BaSO_4$ on the addition of $BaCl_2$ solution. The conversion of COS to $H_2SO_4$ was about 3%. $SO_2$ showed slightly more conversion to $H_2SO_4$. In one day's irradiation about 5% converted. Without HBr, conversion to $H_2SO_4$ by $SO_2$ was negligible. The amount of $BaSO_4$ precipitated was minute. Even elemental $Br_2$ and S, mixed together in water solution showed a high conversion to $H_2SO_4$, but since this reaction occurred in the open air undoubtedy dissolved $O_2$ facilitated the reaction. Therefore, $H_2SO_4$ *is readily produced under postulated Venus atmospheric conditions.*

### 4. Conclusion

The lack of detectable S compounds in the atmosphere of Venus has always been a problem. Whereas the atmosphere of Earth is dominated by $O_2$ and $H_2O$, the Venus atmosphere could be dominated by the halogens. The lack of S is explained by postulating that the clouds of Venus are frozen droplets of 86% $H_2SO_4$, formed by the oxidation of $SO_2$ by elemental $Br_2$ in the upper atmosphere of Venus.

REFERENCES

Beer, R., Norton, R. H., and Martonchik, J. V. 1971, "Absorption by Venus in the 3-4 Micron Region," *Ap. J. Letters,* 168, L121-L124.

Coffeen, D. 1968, "A Polarimetric Study of the Atmosphere of Venus," Ph.D. dissertation, University of Arizona.

Coffeen, D. and Hansen, J. E. 1972, "Polarization Studies of Planetary Atmospheres," a contributed paper to IAU Colloquium 23 on Polarization, University of Arizona.

Fink, U., Larson, H., Kuiper, G. P., and Poppen, R. F. 1972, "Water Vapor in the Atmosphere of Venus," *Icarus,* 17, 617-631.

Gillett, F. C., Low, F. J., and Stein, W. A. 1968,

"Absolute Spectrum of Venus from 2.8 to 14 Microns," *J. Atmos. Sci.,* **25**, 594,595.

Hanel, R., Forman, M. and Stambach, G. 1968, "Preliminary Results of Venus Observations between 8 and 13 Microns," *J. Atmos. Sci.,* **25**, 586-593.

Hansen, J. E. and Arking, A. 1971, "Clouds of Venus: Evidence for their Nature," *Science,* **171**, 669-672.

Kuiper, G. P. 1969, "Identification of the Venus Cloud Layers," *LPL Comm.,* **6**, No. 101, 229-250.

——. 1972. Personal communication; Burch, D. E., Grynak, D. A., Patty, R. R., and Bartky, C. E. 1969, "Absorption of Infrared Radiant Energy by $CO_2$ and $H_2O$. IV. Shapes of Collision-Broadened $CO_2$ Lines," *Jour. Opt. Soc. Amer.,* **59**, 267–280.

Latimer, W. L. 1952, *The Oxidation States of the Elements and their Potentials in Aqueous Solutions,* Prentice-Hall, New York.

Robie, R. A. and Waldbaum, D. R. 1968, *Thermodynamic Properties of Minerals and Related Substances,* G.S.B. 1259, U.S. Govt. Printing Office, Washington.

Wallace, L., Caldwell, J. J. and Savage, B. D. 1972, "Ultraviolet Photometry from the Orbiting Astronomical Observatory. III, Observations of Venus, Mars, Jupiter and Saturn Longward of 2000Å," *Ap. J.,* **172**, 755-769.